Effective theory of relativistic fluids: Hydrodynamic Attractor and Bi-criticality

A Thesis

submitted to
Indian Institute of Science Education and Research Pune
in partial fulfillment of the requirements for the
BS-MS Dual Degree Programme

by

Harish M

Indian Institute of Science Education and Research Pune
Dr. Homi Bhabha Road,
Pashan, Pune 411008, INDIA.

March, 2020

Supervisor: Dr. Ayan Mukhopadhyay

Certificate

This is to certify that this dissertation entitled Effective theory of relativistic fluids: Hydrodynamic Attractor and Bi-criticality towards the partial fulfilment of the BS-MS dual degree programme at the Indian Institute of Science Education and Research, Pune represents study/work carried out by Harish M at the Indian Institute of Technology, Madras, under the supervision of Dr. Ayan Mukhopadhyay, Assistant Professor, Department of Physics , Indian Institute of Technology Madras during the academic year 2019-2020.

Dr. Ayan Mukhopadhyay

Committee:

Dr. Ayan Mukhopadhyay

Dr. Sachin Jain

This thesis is dedicated to my parents

Declaration

I hereby declare that the matter embodied in the report entitled Effective theory of relativistic fluids: Hydrodynamic Attractor and Bi-criticality are the results of the work carried out by me at the Department of Physics, under the supervision of Dr. Ayan Mukhopadhyay at the Indian Institute of Technology, Madras and the same has not been submitted elsewhere for any other degree.

Harish M

Acknowledgments

I am grateful to Prof. Ayan Mukhopadhyay for giving me an opportunity to work with him on this exciting research topic. I thank him for being supportive and encouraging throughout the project. His excitement and knowledge about a wide range of topics in physics has helped me develop a greater appreciation and motivation to explore further. I would also like to thank Prof. Sachin Jain for being a member of my Thesis Committee.

My friends and colleagues Sukrut Mondkar, Toshali Mitra, Tanay Kibe, Hareram Swain, Nehal Mittal, Ankit Anand, and Anshul Mishra at IIT Madras were very helpful during my stay in Chennai. I enjoyed many of the discussions we had over lunch and tea, often with Prof. Mukhopadhyay, on a variety of topics. I especially thank Sukrut for helping me learn computational methods, and his keen interest in my work.

I am thankful to my parents and family for their support throughout my education at IISER Pune, and my friends who played a huge role in making it a wonderful experience to live in Pune. I thank Prof. Arijit Bhattacharyay and Prof. Rajeev Bhalerao at IISER Pune for their support. I was supported by a DST-INSPIRE Grant, the KVPY Fellowship and the INFOSYS Foundation scholarship for my education and research at IISER Pune.

Abstract

We study relativistic hydrodynamics as an effective field theory to describe strongly interacting quantum field theories like QCD at long wavelengths. This approach can be used to model the Quark-Gluon Plasma formed in relativistic heavy-ion collisions with excellent agreement with observations.

The Müller-Israel-Stewart formalism is a phenomenological extension of hydrodynamics which makes the theory causal, unlike finite order hydrodynamics. This introduces certain relaxation modes in the system which lead to the existence of an attractor solution to which the system flows rapidly before reaching equilibrium, even for initial conditions very far away. This is the hydrodynamic behaviour which could explain out of equilibrium fluids and the effectiveness of hydrodynamics in modelling QGP.

Based on observations, to improve models of QGP, weakly interacting modes are coupled to a strongly interacting fluid through effective metrics of the two sectors, in the framework of semi-holography. Such coupled fluids demonstrate a second order phase transition for a particular value of the coupling parameter. The critical behaviour of physical quantities like the entropy, and the hydrodynamic and non-hydrodynamic modes in the total system, is computed to understand the critical behaviour.

Contents

List of Figures

Introduction

Relativistic hydrodynamics is a very effective framework to describe the Quark-Gluon Plasma (QGP), a recently discovered state of matter in relativistic heavy-ion collisions. The QGP, which is governed by strong QCD interactions, behaves as an almost perfect fluid in observations. The system seems to undergo very quick thermalisation to give this fluid like behaviour until the temperature falls below the deconfinement temperature and hadronisation occurs. Understanding this phase of matter and the effectiveness of relativistic hydrodynamics in describing it is a very important problem in Physics.

With this motivation, in chapter 1, we study the general framework of modern hydrodynamics as an effective field theory description of any strongly interacting quantum field theory at large length scales where fluctuations in expectation values are negligible. The effective theory is constructed from symmetry considerations alone by means of a gradient expansion. Successively higher order gradients are assumed to be smaller as fluctuations are long wavelength.

But completing the hydrodynamic theory requires computation of transport coefficients from the underlying theory of QCD. For such strongly interacting fluids, the AdS/CFT correspondence, or more specifically the fluid/gravity duality [1, 2] gives a procedure to do such computations by working in a weakly coupled gravitational dual theory [3, 4, 5]. These computations are otherwise very difficult due to the failure of perturbation theory at strong coupling. Here the microscopic theory is assumed to be described closely by a conformal $\mathcal{N} = 4$ Supersymmetric Yang-Mills theory (this is expected to be true qualitatively for QCD in heavy-ion collisions).

But a pure hydrodynamic theory with a gradient expansion violates causality due to the presence of superluminal propagation [5]. In chapter 2, we see how certain phenomeno-

logically motivated relaxation terms can cure this issue while improving agreement with observations. These terms induce relaxation modes in the system which lead to the recently observed phenomenon of hydrodynamic attractors [6]. The system irrespective of a wide range of initial conditions, flows to a unique attractor solution much before reaching equilibrium. This is a remarkable result which could help develop an understanding of out of equilibrium hydrodynamics, and also explain the effectiveness of the hydrodynamic description of QGP.

The relaxation modes introduced are seen to be non-hydrodynamic modes. The fluid/gravity duality places them analogous to Quasi-Normal Modes in Black Holes. The phenomenological correction made is also seen to be in agreement with the result obtained by the mathematical procedure of Borel resummation of the usually divergent hydrodynamic gradient expansion.

Trying to make improvements to the hydrodynamic description of QGP, some observations indicate the possibility of weakly coupled modes also existing simultaneously with strongly coupled modes in the system (This is expected before the formation of QGP and during hadronisation). In chapter 3, we see a recently developed method to couple such modes using a semi-holographic approach [7, 8]. This allows us to couple two different subsectors in a system with different types of interactions, through couplings between the effective metrics in which these subsectors live. This way, a strongly interacting fluid can be coupled with a weakly interacting kinetic theory to model the QGP and its transition between regimes.

A remarkable second order phase transition has been shown to exist even for the simplest case of two coupled ideal fluids in [7]. This critical behaviour is shown here for coupled MIS fluids, and the rich dynamics near the critical point is explored further. This has important implications for hydrodynamic and non-hydrodynamic modes in the system, and their critical behaviour are derived here. These results are important to understand fluctuations near the critical point especially if stochasticities can also be included (similar to [9]). It could give important consequences when kinetic theories are coupled to MIS fluids to model QGP. It could possibly even be extended to couple black hole solutions.

Chapter 1

Hydrodynamics as an Effective Field Theory

The modern theory of hydrodynamics is developed in a very generic form as a long wavelength effective field theory (reviewed in [10, 11]). For any system, if the fluctuations around equilibrium and transport of conserved quantities occur at a much higher length scale compared to the characteristic length or the mean free path, an effective hydrodynamic description can be constructed for the macroscopic degrees of freedom using the underlying symmetries. The systematic way to proceed is to consider a gradient expansion for the macroscopic conserved quantities, where higher order gradients are succesively smaller because microscopic variations are assumed to exist at long ranges.

For a relativistic system, the expectation values of the Energy-Momentum tensor $T^{\mu\nu}$ and any conserved charges represent the relevant macroscopic variables to be expanded in gradients of local hydrodynamic fields [12]. For a system without any conserved charges, these fields will be a Lorentz scalar a corresponding to the energy, and a Lorentz vector b^{μ} corresponding to the momentum. Thus the symmetric second rank tensor $T^{\mu\nu}$ is to be built from a, b^{μ}, and the metric $g^{\mu\nu}$, treated as the source of perturbations. The dynamical equations for the hydrodynamic fields are the conservation equations

$$\nabla_{\mu} T^{\mu\nu} = 0. \tag{1.1}$$

.

1.1 Zeroth order hydrodynamics

At zeroth order, the fluid is ideal as no fluctuations exist within the system, because all derivatives of the hydrodynamic fields are considered to be zero. In this case, the most general form for $T^{\mu\nu}$ can be seen to be

$$T^{\mu\nu} = a(c_1 b^\mu b^\nu + c_2 g^{\mu\nu}) + f(a)(c_3 b^\mu b^\nu + c_4 g^{\mu\nu}) \tag{1.2}$$

However for the equilibrium system, in the equilibrium frame, from the definition of the energy-momentum tensor and rotational symmetry,

$$T^{\mu\nu} = diag(\epsilon, P, P, P) \tag{1.3}$$

where ϵ is the local energy density, $P(\epsilon)$ is the fluid pressure, and the Minkowski metric is $\eta_{\mu\nu} = diag(-1, 1, 1, 1)$. The form of $P(\epsilon)$ is determined by the equation of state in the microscopic theory. The fluid velocity which is also the time-like eigenvector of $T^{\mu\nu}$ with eigenvalue $-\epsilon$, is here $u^\mu = (1, 0, 0, 0)$. Therefore identifying the timelike eigenvector b^μ of (1.2) with u^μ and its eigenvalue a with ϵ, comparing the form of (1.2) in the Local Rest Frame(LRF) to (1.3), we can solve for the coefficients to get

$$T^{\mu\nu}_{(0)} = (\epsilon + P)u^\mu u^\nu + P g^{\mu\nu} \tag{1.4}$$

To determine the dynamical equations, it is very useful to define the projection operators $\triangle^{\mu\nu} \equiv u^\mu u^\nu + g^{\mu\nu}$ which along with u^μ project the spatial and temporal parts respectively of a tensor. This can be clearly seen in the LRF where u^μ reduces to $(1, 0, 0, 0)$, and $\triangle^{\mu\nu}$ reduces to $diag(0, 1, 1, 1)$. These can be used to project the components of $\nabla_\mu T^{\mu\nu}$, and lead to the relativistic Euler equations

$$D\epsilon + (\epsilon + P)\nabla^\perp_\mu u^\mu = 0, \qquad (\epsilon + P)Du^\mu + c_s^2 \nabla^\mu_\perp \epsilon = 0 \tag{1.5}$$

where $D = u^\mu \nabla_\mu$ and $\nabla^\mu_\perp = \triangle^{\mu\nu}\nabla_\nu$ are the co-moving temporal and spatial derivatives respectively, and $c_s = \sqrt{\partial P(\epsilon)/\partial\epsilon}$ is the thermodynamic speed of sound.

With the entropy density S defined thermodynamically by,

$$\epsilon + P = TS \tag{1.6}$$

the entropy current J^μ defined below can be seen to be divergenceless, showing how the ideal flow doesn't produce any entropy.

$$J^\mu = Su^\mu, \quad \nabla_\mu J^\mu = 0 \tag{1.7}$$

1.2 First Order Hydrodynamics

To include out of equilibrium effects like viscosity, it is necessary to move to higher orders in the hydrodynamic gradient expansion. First order hydrodynamics makes corrections to the ideal fluid by including first order covariant derivatives of the hydrodynamic fields ϵ, and u^μ, and their combinations (the covariant derivative of the metric vanishes, and $P = P(\epsilon)$). Similar to the case of ideal fluids, u^μ is defined again as the timelike eigenvector of $T^{\mu\nu}$ in the Landau frame for the out of equilibrium system. This poses restrictions on the form of the higher order correction $\Pi^{\mu\nu}$ to the stress tensor, because $u_\mu T^{\mu\nu}_{(0)} = -\epsilon u^\nu$ holds already, which forces $u_\mu \Pi^{\mu\nu} = 0$. This is because we can use lower order equations to make simplifications at higher orders when solving the system order by order.

The components of $\nabla_\mu \epsilon$ and $\nabla_\mu u_\nu$ can be projected out using the projectors and the zeroth order Euler equations then show that the only independent terms are the spatial dertivatives $\nabla^\perp_\mu \epsilon$ and $\nabla^\perp_\mu u_\nu$. However, to create the symmetric second rank tensor $T^{\mu\nu}_{(1)}$ (the first order terms in $T^{\mu\nu}$) satisfying $u_\mu T^{\mu\nu}_{(1)} = 0$, the possible terms are $\triangle^{\mu\nu}\nabla_\rho u^\rho$ and $\nabla^\perp_{(\mu} u_{\nu)}$, which is the symmetric combination of $\nabla^\perp_\mu u_\nu$ and $\nabla^\perp_\nu u_\mu$.

A linear combination of these terms which separates the traceless part of $T^{\mu\nu}_{(1)}$ is given by

$$\triangle^{\mu\nu}\nabla_\rho u^\rho, \quad \sigma^{\mu\nu} = 2\nabla^{<\mu} u^{\nu>} = 2\nabla^{(\mu}_\perp u^{\nu)} - \frac{2}{d-1}\triangle^{\mu\nu}\nabla_\rho u^\rho \tag{1.8}$$

where d is the dimension of the space-time. This is useful especially when moving to conformal fluids later. $\sigma^{\mu\nu}$ is the traceless part of $T^{\mu\nu}_{(1)}$, which can now be written as

$$T^{\mu\nu}_{(1)} = -\eta\sigma^{\mu\nu} - \zeta\triangle^{\mu\nu}\nabla_\rho u^\rho \tag{1.9}$$

The transport coefficients η and ζ are the coefficients of shear viscosity and bulk viscosity respectively, which have to be computed from the underlying theory.

The Ward Identity now gives the relativistic Navier-Stokes Equations

$$D\epsilon + (\epsilon + P)(\nabla^{\perp}_{\rho} u^{\rho}) = \frac{\eta}{2}\sigma^{\mu\nu}\sigma_{\mu\nu} + \zeta(\nabla^{\perp}_{\rho} u^{\rho})^2 \tag{1.10}$$

$$(\epsilon + P)Du^{\rho} + c_s^2 \nabla^{\rho}_{\perp}\epsilon = \triangle^{\rho}_{\mu}\nabla_{\nu}(\eta\sigma^{\mu\nu} + \zeta\triangle^{\mu\nu}\nabla^{\perp}_{\lambda}u^{\lambda}) \tag{1.11}$$

This process of determining the most general form of the gradient expansion can be continued in principle to any finite order to improve the accuracy of the approximation. However as mentioned in the next section, there is a causality issue associated which impedes the computational utility of these finite order descriptions. The summation is also possibly not well-defined if the expansion diverges (which is shown to be the case very often, in [13]). These two issues are avoided by phenomenological modifications to the theory or the process of Borel Resummation. These are explained in detail in section 2.2, and 2.8, and both of these are seen to lead to equivalent results in section 2.8.

1.3 Causality issue of finite order hydrodynamics

At any finite order in hydrodynamics, causality is violated. This can be seen from the first order Navier-Stokes equations (1.10) which contain only first derivatives in time while spatial derivatives occur upto second order. So this is a parabolic system of differential equations without a well-defined initial value problem since any perturbations to the initial conditions propagate instantaneously [5]. This is an issue when numerically evolving a system as it might move out of the light-cone because of the superluminal propagation.

This is easy to see in the simpler case of diffusion in a fluid with a single conserved charge, discussed in the next section. The straightforward cure for this issue is to add phenomenological terms which make any fluctuations in the system exponentially decay rather than propagate instantaneously. This procedure is shown in section 1.4 for diffusion, and in section 2.2 for first-order hydrodynamics. These terms produce relaxation modes with characteristic time scales of decay in both the cases, which help to restore causality.

1.4 Diffusion in a fluid

For a diffusive system in Minkowski background with a single conserved charge ρ, the dynamical equation is the continuity equation

$$\partial_\mu j^\mu = \partial_t \rho + \nabla \cdot \mathbf{j} = 0 \tag{1.12}$$

$j^\mu = (\rho, \mathbf{j})$ is the current density associated with the flow of charge ρ. Analogous to the hydrodynamic expansion, we can write $\mathbf{j}$ in a derivative expansion of the fundamental conserved charge ρ. No zeroth order term is possible as $\mathbf{j}$ is a vector and ρ is a scalar. At first order, we get

$$\mathbf{j}_{(1)} = -D\nabla\rho \tag{1.13}$$

where the diffusion constant D is a transport coefficient. (1.12) gives the diffusion equation

$$\partial_t \rho - D\nabla^2 \rho = 0 \tag{1.14}$$

This is again a parabolic equation similar to first order hydrodynamics. Adding higher derivative terms of ρ clearly doesn't resolve this issue. The fourier transform of (1.14) gives the dispersion relation of the diffusive mode

$$\omega = -iDk^2. \tag{1.15}$$

A group velocity could be defined as $v_g = d|\omega|/dk$, and then it can be seen to be larger than 1 for large k ($k > 1/2D$). This shows the diffusive spreading of a perturbation could be acausal.

A possible solution is to include a phenomenological term which gives a rapid decay of any fluctuations around the equilibrium,

$$\mathbf{j} = -D\nabla\rho - \tau\partial_t \mathbf{j} \tag{1.16}$$

This ensures that when $\nabla\rho = 0$, $\mathbf{j}$ decays exponentially. This expression can be expanded iteratively to higher orders. However it can be seen that this iterative expansion is not identical to the gradient expansion because it does not contain any nonlinear terms like $\nabla(\nabla\rho \cdot \nabla\rho)$ which occur in the general gradient expansion at higher orders. So this process

can be thought of as a resummation, which is later explained in section 2.8.

The diffusion equation is now

$$\partial_t \rho - D\nabla^2 \rho + \tau \partial_t^2 \rho = 0 \tag{1.17}$$

This is easily verified to be a hyperbolic differential equation with second order time derivatives also, and hence it does not have a causality issue. The dispersion relation is different in this case, with the two modes given as

$$\omega = -\frac{i}{2\tau} \pm \sqrt{-\frac{1}{4\tau^2} + \frac{Dk^2}{\tau}} \tag{1.18}$$

This leads to the very interesting and important consequence of the existence of non-hydrodynamic modes. The modes in finite order diffusion or hydrodynamics (as seen in 1.15 and later in section 2.7) are such that $\omega \to 0$ as $k \to 0$ (the hydrodynamic limit) which is indicative of the fact that long wavelength modes carry low energies. However from (1.18), along with the usual diffusive mode (1.15), we get a new non-hydrodynamic mode which does not go to 0 in the $k \to 0$ limit.

$$\omega = -iDk^2, \quad \omega = -\frac{i}{\tau} \tag{1.19}$$

The new relaxation mode $\omega = -i/\tau$ is responsible for rapid decay of fluctuations in the system, making the system causal. They remain finite even in the long wavelength hydrodynamic limit unlike the hydrodynamic modes which die off. We are interested in this limit because hydrodynamics is a long wavelength theory, and clearly the relaxation modes have a very large contribution in this regime.

This description agrees well with observations in diffusive systems, where fluctuations do decay very rapidly. Such a decaying mode also occurs in hydrodynamics on the addition of an analogous relaxation term to the hydrodynamic expansion (section 2.2), and has very important consequences leading to the hydrodynamic attractor (section 2.8). In the context of the fluid/gravity duality, they have also been shown to be analogous to Quasi-Normal Modes in Black Holes. So they could also provide important qualitative insights into black holes.

Chapter 2

Hydrodynamic Attractor

The hydrodynamic attractor is a recently observed phenomena in fluids which sheds important information on the effectiveness of hydrodynamics in describing systems like the QGP. The crux of the result is the existence of an attractor solution to which the fluid flows even when far from equilibrium [6]. This shows the process of thermalisation in out-of-equilibrium fluids.

The result was observed for a system obeying the Müller-Israel-Stewart (MIS) theory [14, 15] (seen in section 2.2), specifically in a type of fluid flow called the Bjorken flow [16] commonly used to model Relativistic Heavy-Ion Collisions. This makes it a good model to possibly describe the dynamics of QGP formed in these collisions. The non-hydrodynamic mode from the MIS theory is also seen to play a very crucial role in the existence of the attractor by forcing decay of fluctuations around this solution. Another assumption commonly used is to treat the fluids as conformally invariant. This allows several simplifications to the model and enables the use of the AdS/CFT correspondence in computing transport coefficients for the strongly interacting fluid [3, 4]. These preliminaries required and the attractor solution are explained in the next sections.

2.1 Conformal Fluids

Confromal fluids (reviewed in [5, 10, and 11])are defined to be conformally invariant, or more specifically, invariant under a Weyl transformation of the metric,

$$g_{\mu\nu} = e^{2\phi}\tilde{g}_{\mu\nu}. \tag{2.1}$$

We require the relevant physical quantities and equations to be Weyl invariant so that the theory is also Weyl invariant. A tensor $Q^{\mu_1\cdots\mu_n}_{\nu_1\cdots\nu_m}$ is said to transform homogenously or called Weyl invariant, with a conformal weight ω, if under the Weyl transformation of the metric given by (2.1), it transforms as

$$Q^{\mu_1\cdots\mu_n}_{\nu_1\cdots\nu_m} = e^{-\omega\phi}\tilde{Q}^{\mu_1\cdots\mu_n}_{\nu_1\cdots\nu_m} \tag{2.2}$$

From the definition of the inverse metric $g^{\mu\nu}$, and the normalisation of the fluid velocity $u^\mu u_\mu = -1$, it can be seen that

$$g^{\mu\nu} = e^{-2\phi}\tilde{g}^{\mu\nu}, \quad u^\mu = e^{-\phi}\tilde{u}^\mu \tag{2.3}$$

To find the transformation rule for the energy-momentum tensor $T^{\mu\nu}$, we use the requirement that the dynamical conservation rule (1.1) should remain invariant. This can then be shown (appendix D of [17]) to imply

$$g_{\mu\nu}T^{\mu\nu} = 0, \quad T^{\mu\nu} = e^{-(d+2)\phi}\tilde{T}^{\mu\nu}, \tag{2.4}$$

i.e., $T^{\mu\nu}$ is traceless, and transforms with a conformal weight of (d+2) where d is the dimension of the space-time. This poses restrictions on the form of $T^{\mu\nu}$ for conformal fluids. The tracelessness condition applied at the zeroth order implies

$$\epsilon = (d-1)P \tag{2.5}$$

This relation provides the equation of state $P(\epsilon)$ and fixes the speed of sound $c_s = \sqrt{dP/d\epsilon}$ as a dimension dependent quantity,

$$c_s = \frac{1}{\sqrt{d-1}} \tag{2.6}$$

Going to first order hydrodynamics in conformal fluids, only the the shear term $\sigma^{\mu\nu}$ can contribute to $T^{\mu\nu}$ as it is traceless, while the bulk viscosity term will not be present because it has a non-zero trace. These modifications simplify the study of conformal fluids considerably and allows the system to be thought of as having a microscopic theory like the $\mathcal{N} = 4$ SYM model, which in turn makes it possible to use the fluid/gravity duality to perform microscopic computations. Going ahead we will be exclusively studying conformal fluids though many of the results obtained can, and have been generalised to non-conformal fluids. But an important requirement is to consistently use Weyl invariant quantities and equations. This does not occur for terms with the ordinary covariant derivative as discussed below. So a new generalisation to the covariant derivative is required. This is done in the Weyl covariant formalism [18].

2.1.1 Weyl covariant formalism

The usual covariant derivative of a tensor does not transform homogenously under a Weyl Transformation. This is explicitly seen for the derivative of u^μ

$$\nabla_\mu u^\nu = e^{-\phi}(\tilde{\nabla}_\mu \tilde{u}^\nu + \delta^\nu_\mu \tilde{u}^\rho \partial_\rho \phi - \tilde{g}_{\mu\rho}\tilde{u}^\rho \tilde{g}^{\nu\sigma}\partial_\sigma \phi) \tag{2.7}$$

But for a tensor $Q^{\mu\cdots}_{\nu\cdots}$ which transforms homogenously with a conformal weight ω, it is possible to define the Weyl covariant derivative which also transforms with the same conformal weight ω under a Weyl transformation as below

$$\begin{aligned}\mathcal{D}_\lambda Q^{\mu\cdots}_{\nu\cdots} = \nabla_\lambda Q^{\mu\cdots}_{\nu\cdots} + \omega A_\lambda Q^{\mu\cdots}_{\nu\cdots} + (g_{\lambda\alpha}A^\mu - \delta^\mu_\lambda A_\alpha - \delta^\mu_\alpha A_\lambda)Q^{\alpha\cdots}_{\nu\cdots} + \cdots \\ -(g_{\lambda\nu}A^\alpha - \delta^\alpha_\lambda A_n u - \delta^\alpha_\nu A_\lambda)Q^{\mu\cdots}_{\alpha\cdots} + \cdots\end{aligned}$$

where requiring the following two conditions

$$\mathcal{D}_\mu u^\mu = 0, \quad u^\mu \mathcal{D}_\mu u^\nu = 0 \tag{2.8}$$

fixes uniquely the form of A_μ as

$$A_\mu = u^\lambda \nabla_\lambda u_\mu - \frac{1}{d-1} u_\mu \nabla_\lambda u^\lambda \tag{2.9}$$

This Weyl covariant derivative can be used to replace the usual covariant derivative in the hydrodynamic theory to ensure that all the physical variables like $\sigma^{\mu\nu}$ and dynamical equations like the conservation equations are Weyl invariant. It can also be shown that for $T^{\mu\nu}$, the Weyl covariant derivative is equivalent to the usual covariant derivative and is 0. Hence this formalism is very useful to study the dynamics of conformal fluids.

2.2 The Müller-Israel-Stewart formalism

Analogous to the gradient expansion in diffusion, a phenomenological term is added to the hydrodynamic expansion in the Müller-Israel-Stewart (MIS) theory [12, 13] with the intention of resolving the causality violation. Upto first order, the correction $\Pi^{\mu\nu}$ to the ideal fluid energy-momentum tensor is [5]

$$\Pi^{\mu\nu} = -\eta\sigma^{\mu\nu} - \tau_{\Pi} u^{\rho}\mathcal{D}_{\rho}\Pi^{\mu\nu} \tag{2.10}$$

(There is no bulk viscosity term because as mentioned earlier we are continuing to work with conformal fluids)

Here $\Pi^{\mu\nu}$, called the MIS field, is treated as a new independent field in the system which obeys the dynamical equation (2.10). This MIS field is responsible for the decay of fluctuations and the non-hydrodynamic modes discussed later in section 2.7. This construction can also be done at higher orders in hydrodynamics by adding an appropriate relaxation term to the finite order stress tensor (second order MIS theory is considered in section 2.4).

2.3 Bjorken Flow

Bjorken flow [14] is a special case very often used in Relativistic Heavy-Ion Collisions to model QGP dynamics. The fluid is assumed to flow only in one longitudinal direction - usually chosen to be z. It is assumed to be homogenous with infinite extent in the x and y directions and hence the flow is independent of these directions. The flow is also assumed to be boost invariant in the z-direction. Though this is a very simplified model, it still gives many important results about the hydrodynamic behaviour, and is very relevant for

understanding experimental observations.

We assume the fluid to live in the flat Minkowski background, but the symmetries of the system makes it convenient to go to the Milne co-ordinates (τ, x, y, ξ) defined by

$$\tau \equiv \sqrt{t^2 - z^2}, \quad \xi \equiv arctanh(\frac{z}{t}) \tag{2.11}$$

where τ is the proper time, and ξ the rapidity. In these new co-ordinates, using the transformation rules for tensors, it can be shown that

$$u^\mu = (1, 0, 0, 0), \quad g^{\mu\nu} = diag(-1, 1, 1, \tau^2) \tag{2.12}$$

The spatial components being zero and the time component being identity for u^μ means that in the Milne co-ordinates, the fluid is at rest, while the form of $g^{\mu\nu}$ is that of an expanding space-time in the z-direction. Thus going to the Milne co-ordinates allows us to reinterpret the system as a fluid at rest in a space-time which is expanding longitudinally rather than an expanding fluid in a static metric. In these co-ordinates, the Christoffel symbols are computed to show that the only two non-zero components are,

$$\Gamma^\xi_{\xi\tau} = 1/\tau, \quad \Gamma^\tau_{\xi\xi} = \tau \tag{2.13}$$

The Riemann tensor is zero as expected because the background is Minkowski.

This redefinition allows us to simplify the study of the Bjorken flow even further because all variables are dependent only on the single co-ordinate τ, the proper time. Though we will work with the Bjorken flow to calculate the attractor as done in the original work of Heller and Spalinski [6], later works have shown similar attractor solutions in some other fluid flows also.

2.4 Second order MIS theory

Following the original computation of the attractor in [7], we consider a strongly interacting fluid in Bjorken flow obeying a second order MIS theory. Here, the modification to the zeroth order stress tensor includes upto second order hydrodynamic gradients along with a relaxation term.

With the restrictions on the correction $\Pi^{\mu\nu}$ that it should be symmetric, $u_\mu \Pi^{\mu\nu} = 0$ in the Landau Frame, and $g_{\mu\nu}\Pi^{\mu\nu} = 0$ because of conformal invariance, eight possible second order terms can be constructed. However only five combinations of these transform homogenously under the Weyl transformation. These along with the first order shear term give the most general form of $\Pi^{\mu\nu}$ [5]

$$\begin{aligned}\Pi^{\mu\nu} = -\eta\sigma^{\mu\nu} - \tau_\Pi \, {}^{\langle}\mathcal{D}\Pi^{\mu\nu\rangle} + \kappa \left[R^{\langle\mu\nu\rangle} - (d-2)u_\rho R^{\rho\langle\mu\nu\rangle\sigma}u_\sigma\right] \\ + \frac{\lambda_1}{\eta^2}\Pi^{\langle\mu}{}_\rho \Pi^{\nu\rangle\rho} - \frac{\lambda_2}{\eta}\Pi^{\langle\mu}{}_\rho\Omega^{\nu\rangle\rho} + \lambda_3\Omega^{\langle\mu}{}_\rho\Omega^{\nu\rangle\rho}\end{aligned}$$

Here τ_Π is the phenomenological parameter which dictates the time-scale of the decay of fluctuations, and κ, λ_1, λ_2, and λ_3 are various transport coefficients. $\mathcal{D}$ is defined as $u_\mu \mathcal{D}^\mu$, and for a second rank tensor $Q^{\mu\nu}$,

$$Q^{\langle\mu\nu\rangle} = {}^{\langle} Q^{\mu\nu\rangle} = \frac{1}{2}\triangle^{\mu\rho}\triangle^{\nu\sigma}(Q_{\rho\sigma} + Q_{\sigma\rho}) - \frac{1}{d-1}\triangle^{\mu\nu}\triangle^{\rho\sigma}Q_{\rho\sigma} \tag{2.14}$$

$R^{\mu\nu\rho\sigma}$ is the Riemann tensor, $R^{\mu\nu}$ the Ricci tensor, and $\Omega^{\mu\nu}$ the vorticity defined as

$$\Omega^{\mu\nu} = \frac{1}{2}\triangle^{\mu\rho}\triangle^{\nu\sigma}(\mathcal{D}_\rho u_\sigma - \mathcal{D}_\sigma u_\rho) \tag{2.15}$$

However as we are interested in the case of Bjorken flow in the Milne co-ordinates, the Riemann tensor is zero, and $\mathcal{D}_\mu u^\mu = 0$, so the flow is irrotational and the vortcity is zero. Therefore, in our case, the MIS equation reduces to

$$\Pi^{\mu\nu} = -\eta\sigma^{\mu\nu} - \tau_\Pi \, {}^{\langle}\mathcal{D}\Pi^{\mu\nu\rangle} + \frac{\lambda_1}{\eta^2}\Pi^{\langle\mu}{}_\lambda \Pi^{\nu\rangle\lambda} \tag{2.16}$$

2.5 Transport coefficients from Fluid-gravity duality

For completely understanding a hydrodynamic theory, computing the transport coefficients from the underlying theory is important. For strongly interacting fluids, the AdS/CFT correspondence provides a way to do this computation.

In [1], the AdS/CFT correspondence has been used to show a more specific duality between strongly interacting conformal fluids and certain black hole solutions, known as

the fluid/gravity duality. This duality allows us to do computations in gravity which are relatively simple, as compared to strongly interacting theories like $\mathcal{N} = 4$ SYM theory (which in many qualitative aspects resemble QCD) where perturbation theory breaks down. Thus it allows us to look into a regime otherwise difficult to explore. It could also possibly have more general applications in understanding problems in fluid dynamics like turbulence, or problems in black holes like Quasi-Normal Modes. It is used very commonly in the context of modelling QGP because of the strong QCD interactions which determine its dynamics.

In the case of the MIS system, the fluid/gravity duality has been used to compute the transport coefficients in the theory [3, 4, 5]

$$\tau_\Pi = \frac{C_{\tau_\Pi}}{T}, \quad \lambda_1 = C_{\lambda_1}\frac{\eta}{T}, \quad \eta = C_\eta s \tag{2.17}$$

where T is the temperature, and s the entropy density. For $\mathcal{N} = 4$ SYM theory, the constants above have been computed (reviewed in [12])

$$C_{\tau_\Pi} = \frac{2 - log2}{2\pi}, \quad C_\eta = \frac{1}{4\pi}, \quad C_{\lambda_1} = \frac{1}{2\pi} \tag{2.18}$$

2.6 The Attractor solution

The attractor was shown in [6] by studying the dynamical evolution of the MIS system and finding the trajectory of the fluid for a range of initial conditions of the system. For the conformal Bjorken flow following the MIS theory, the dynamical equations are given by the conservation equations (1.1) and the MIS equations (2.16). But a simplification of the form of the MIS field $\Pi^{\mu\nu}$ can be done using the conformal symmetry and symmetries of the Bjorken flow. In the Milne co-ordinates, the symmetry of the flow implies that $\Pi^{\mu\nu}$ is diagonal while the Landau frame condition $u_\mu\Pi^{\mu\nu} = 0$ requires $\Pi^{\tau\tau}$ to be zero. $\Pi^{xx} = \Pi^{yy}$ again from symmetry, and tracelessness of $\Pi^{\mu\nu}$ requires that it has only one independent component

$$\phi = -\Pi^\xi_\xi = 2\Pi^x_x = 2\Pi^y_y \tag{2.19}$$

The first dynamical equation, the ward identity (1.1) gives

$$\tau\dot{\epsilon} = -\frac{4}{3}\epsilon + \phi \tag{2.20}$$

and the MIS equation (2.16) gives,

$$\tau_\Pi \dot{\phi} = \frac{4\eta}{3\tau} - \frac{\lambda_1 \phi^2}{2\eta^2} - \frac{4\tau_\Pi \phi}{3\tau} - \phi \tag{2.21}$$

Here the dot above a variable refers to a proper time derivative. From (2.20), ϕ can be substituted in (2.21) to get a single second-order differential equation in $\epsilon(\tau)$. Using the relation $\epsilon(T) \sim T^4$ in a 4-dimensional conformal system, this can be further rewritten as a second order equation in $T(\tau)$. Assuming $\lambda_1 = 0$ for simplicity to avoid non-linear terms (this is equivalent to using the first order MIS equation),

$$\tau C_{\tau_\pi} \frac{\ddot{T}}{T} + 3\tau C_{\tau_\Pi} \left(\frac{\dot{T}}{T}\right)^2 + \left(\frac{11 C_{\tau_\pi}}{3T} + \tau\right) \dot{T} - \frac{4}{9\tau}(C_\eta - C_{\tau_\pi}) + \frac{T}{3} = 0 \tag{2.22}$$

(2.22) can be reformulated in terms of the dimensionless quantities [6]

$$\omega = \tau T, \quad f = \frac{\tau \dot{\omega}}{\omega}. \tag{2.23}$$

Since conformal symmetry involves scale invariance, dimensionless quantities are physically relevant, and this change also gives a first order equation,

$$C_{\tau_\pi} \omega f f' + 4 C_{\tau_\Pi} f^2 + \left(\omega - \frac{16}{3} C_{\tau_\Pi}\right) f - \frac{4}{9}(C_\eta + \frac{16}{9} C_{\tau_\pi}) - \frac{2\omega}{3} = 0 \tag{2.24}$$

where a dash over a variable indicates a derivative with respect to ω.

This equation was solved numerically in [6] with appropriate initial conditions relevant to the QGP fireball conditions to plot trajectories on the $f - w$ plane. The result is reproduced below in Fig. 2.1. for qualitative understanding. It can be seen that irrespective of a wide range of initial conditions, the numerical solutions of (2.24) - the blue curves, tend to flow to a single attractor - the black curve, before reaching equilibrium - the red curve. The green curve corresponds to the first order hydrodynamic solution.

Any finite order hydrodynamic theory has a single solution instead of a family of curves because of the lack of the independent MIS variable ϕ. This leads to a first order equation in $T(\tau)$ and a polynomial solution in $1/\omega$ for $f(\omega)$. These solutions are

$$f_{(0)}(\omega) = \frac{2}{3}, \quad f_{(1)}(\omega) = \frac{2}{3} + \frac{4 C_\eta}{9\omega} \tag{2.25}$$

and so on, with the next higher order term in $1/\omega$ appearing at the next order in hydrodynamics. Here $f_{(n)}$ is used to note the solution for nth order hydrodynamics.

The numerical attractor solution (the black curve) is found by taking the $\omega \to 0$ limit of (2.24), and estimating the value of $f(\omega \to 0)$.

$$\lim_{\omega \to 0} f(\omega) = \frac{2\sqrt{C_{\tau_\Pi}} + \sqrt{C_\eta}}{3\sqrt{C_{\tau_\Pi}}} \tag{2.26}$$

This relation is used as the initial condition to numerically solve (2.24) and get the black curve. This curve extends the attractor solution to very small values of ω.

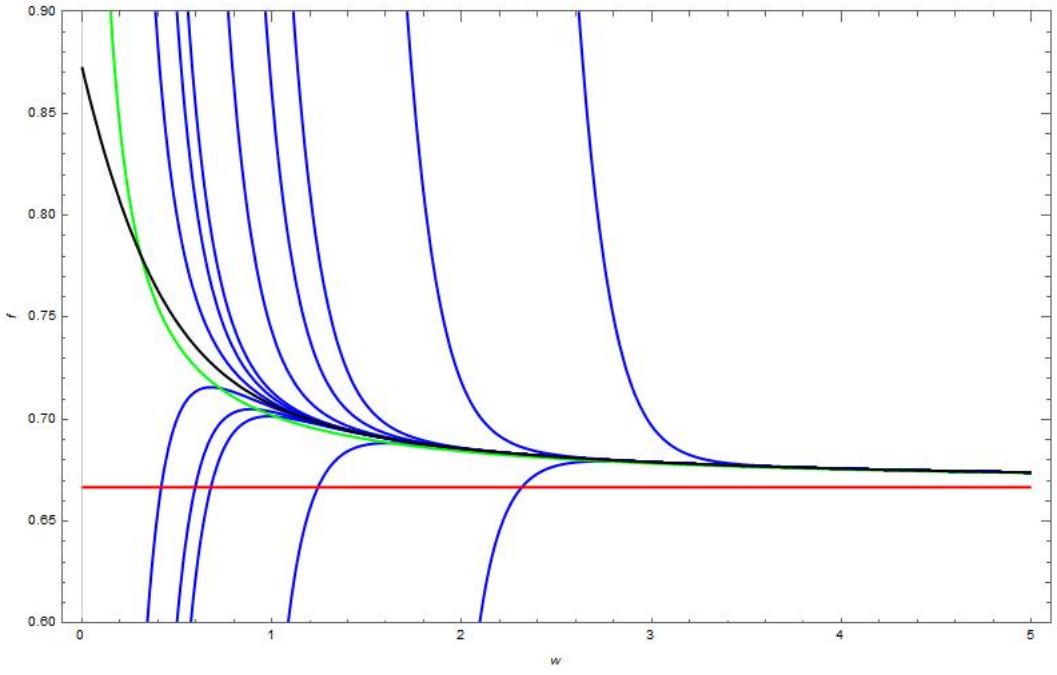

Figure 2.1: *Attractor solution plot $f - \omega$.* The blue lines are numerically obtained solutions for various initial conditions, the black line is obtained using the initial condition for f at small ω (2.26), the red line is from ideal hydrodynamics (equilibrium), and the green line is from first order hydrodynamics.

The MIS solution (2.24) can also be perturbatively solved for f in orders of $1/\omega$ because the system has smaller gradients at late times τ, or when ω is large. We can remarkably recover the entire hydrodynamic gradient expansion upto any finite order [6] by this method

and can be verified at higher orders.

$$f(\omega) = \frac{2}{3} + \frac{4C_\eta}{9\omega} + \frac{8C_\eta C_{\tau_\Pi}}{27\omega^2} + \mathcal{O}\left(\frac{1}{\omega^3}\right) \tag{2.27}$$

This shows that similar to the modified diffusion scenario, even though the relaxation term does not capture all the possible terms in the hydrodynamic gradient expansion of $T^{\mu\nu}$, it still can be thought of as a resummed version of the expansion [6] which removes the divergence issue but captures the hydrodynamic behaviour completely . This is a remarkable result further justified using the formal definition of Resummation in section 2.8.

The attractor solution suggests that the fluid irrespective of large fluctuations, tends to damp down quickly to the attractor before finally reaching equilibrium. This has been defined to be the 'hydrodynamic behaviour' by Heller and Spalinski in [6]. This process of hydrodynamisation could explain the effectiveness of hydrodynamics in various systems like QGP. It could also be studied further to possibly understand the theory of out of equilibrium thermodynamics. The fact that the attractor exists even for extremely small values of ω (the black curve with initial condition from (2.26)) further justifies this because finite order hydrodynamic expansions of f in $1/\omega$ are otherwise expected to break down at small ω (as the hydrodynamic approximation is expected to break down at small times due to large fluctuations).

The decay of fluctuations away from the attractor is due to the non-hydrodynamic modes in the theory (section 2.7). A small perturbation around the attractor solution can be seen to die off [6] as

$$\delta f(\omega) = e^{-\frac{3\omega}{2C_{\tau_\Pi}}}\omega^{\frac{C_\eta - 2C_{\lambda_1}}{C_{\tau_\Pi}}}\left(1 + \mathcal{O}(\frac{1}{\omega})\right) \tag{2.28}$$

This is shown in [6] to agree with the results of Borel resummation of the hydrodynamic gradient expansion (section 2.8).

2.7 Hydrodynamic and non-hydrodynamic modes

An important aspect of the theory we are interested in is the response of the system to small fluctuations around equilibrium. We introduce small perturbations to the equilibrium

stress tensor and see the linear response of the system to these changes [5]. The conservation equations can then be solved perturbatively, and using the zeroth order relation, we get the propagation modes for the fluctuations.

We have many possible components of the stress tensor to introduce fluctuations in. But we can note that the system has spatial rotational invariance in three dimensions (the equilibrium breaks Lorentz invariance). If we choose the propagation of the modes to be along a particular direction, say z, then the rotational invariance reduces to only the x-y plane. So any perturbation along z would behave as a scalar and we call this the sound sector of perturbations, since the fluctuations are along the propagation direction . But any perturbation on the x-y plane behaves as a vector and forms the shear sector, since the perturbation is orthogonal to the propagation direction. Thus we find the perturbations categorised into different sectors, and the shear and sound sectors are explored for an MIS fluid in the next sections.

2.7.1 Shear Sector

In the shear sector, if the propagation direction is along z, the perturbations lie in the x-y plane. For simplicity, we assume they are along the x-direction. So even though in equilibrium the normalised fluid velocity $u^\mu = (1, 0, 0, 0)$, we introduce a perturbation $\delta u^x \sim e^{i(\omega t - kz)}$ (any other perturbation is also assumed to have such a form). So we expect a shear viscosity term with xz component, and include the MIS field Π^{xz} to capture this. With just these perturbations to the equilibrium, we can derive the Ward identity (1.1) and the MIS equation (2.10) for the system. Assuming the equilibrium energy density and pressure to be ϵ and P respectively, we can use the zeroth order equations for simplification.

$$\nabla_\mu T^{\mu\nu} = 0,\ \nabla_\mu T^{\mu\nu}_{(0)} = 0 \quad \Rightarrow \quad \nabla_\mu \delta T^{\mu\nu} = 0 \tag{2.29}$$

where $\delta T^{\mu\nu}$ is the perturbation to the equilibrium stress tensor $T^{\mu\nu}_{(0)}$. (2.29) gives

$$(\epsilon + P)\partial_t \delta u^x + \partial_z \Pi^{zx} = 0 \tag{2.30}$$

and with a fourier transform of (2.30) we get

$$\omega(\epsilon + P)\delta u^x + k\Pi^{zx} = 0 \tag{2.31}$$

Similarly from the MIS equation (2.10), we get

$$\tau_\Pi \partial_t \Pi^{zx} + \Pi^{zx} = -\eta \partial_z \delta u^x \tag{2.32}$$

which after fourier transform gives

$$(1 - i\omega\tau_\Pi)\Pi^{zx} = ik\eta\delta u^x \tag{2.33}$$

From (2.31) and (2.33), the perturbations δu^x and Π^{zx} can be eliminated to derive

$$\omega^2\tau_\Pi + i\omega - k^2\frac{\eta}{(\epsilon + P)} = 0 \tag{2.34}$$

The solutions to (2.34) give the dispersion relation in the shear sector. In the hydrodynamic limit, i.e., $k \to 0$ (where hydrodynamics works well as it is a long wavelength theory), we get two solutions

$$\omega_h = -i\frac{\eta}{(\epsilon + P)}k^2, \quad w_n = -\frac{i}{\tau_\Pi} \tag{2.35}$$

Here the mode ω_h is a hydrodynamic mode because it dies off in the hydrodynamic limit, but the new mode ω_n is a non-hydrodynamic mode beacuse it remains finite at the hydrodynamic limit. From the form of ω_n, it is clear that this mode arises as a result of the relaxation term in the MIS field. So this mode is responsible for the rapid decay of fluctuations near the attractor. The hydrodynamic mode meanwhile has a form closely resembling the diffusion mode with a dependence on k^2. These results will later be rederived for coupled fluids in section 3.4 to see a very similar structure.

2.7.2 Sound Sector

In the sound sector, perturbations to the system are along the direction of propagation, z. Here we can have perturbations to diagonal components of the stress tensor and hence we assume a possible perturbation $\delta\epsilon$ to the equilibrium energy density ϵ. This gives a perturbation $\delta P = c_s^2\delta\epsilon$ to the equilibrium pressure P. The perturbation to the fluid velocity is also along the z direction, δu^z. The only possible non-zero component of the MIS field is Π^{zz} due to the rotational symmetry in the x-y plane. As in the case of the shear sector, we

can derive the correction to the ward identity (1.1) using the equilibrium relation to get

$$\partial_t \delta\epsilon + (\epsilon + P)\partial_z \delta u^z = 0, \quad (\epsilon + P)\partial_t \delta u^z + c_s^2 \partial_z \delta\epsilon + \partial_z \Pi^{zz} = 0 \tag{2.36}$$

The MIS equation (2.10) gives the relation

$$\tau_\Pi \partial_t \Pi^{zz} + \Pi^{zz} + \frac{2(d-2)}{d-1}\eta \partial_z \delta u^z = 0 \tag{2.37}$$

Similar to the shear channel, the fourier transforms of (2.36) and (2.37) can be used to eliminate the perturbations and derive the dispersion relation. In the hydrodynamic limit, we get the modes

$$\omega_\pm = \pm c_s k - i\Gamma k^2, \quad \omega_n = -\frac{i}{\tau_\Pi} \tag{2.38}$$

The modes $\omega_\pm$ are hydrodynamic modes since they vanish in the hydrodynamic limit. Here Γ is the attenuation constant given by

$$\Gamma = \frac{\eta}{\epsilon + P}\frac{d-2}{d-1} \tag{2.39}$$

We again get the same non-hydrodynamic mode ω_n as in the case of the shear sector. This is to be expected because by definition these are modes which exist independent of the propagation vector $\mathbf{k}$ and hence are independent of the choice of different sectors based on the orientation of $\mathbf{k}$. This mode as mentioned earlier is responsible for the attractor due to the rapid decay of fluctuations. Later, in section 3.6, these modes are also studied in a system of coupled MIS fluids to understand the critical point in the system better.

2.8 Borel resummation

In [6], the method of Borel resummation is shown to be a very effective tool in understanding the hydrodynamic expansion and the attractor. The hydrodynamic gradient expansion is shown to be in general divergent in [13]. However in [6], this expansion is shown to be Borel resummable in a generalised way, which allows us to get meaningful results from the expansion. The exact definition is clearly described in [10] through an example. This is explained below for clarity.

$f(x)$ defined by the power series

$$f(x) = \sum_{n=0}^{\infty} (-1)^n n! x^n \tag{2.40}$$

is divergent. The Borel transform of a function $g(x) = \sum_{n=0}^{\infty} k_n x^n$ is defined as $g_B(x) = \sum_{n=0}^{\infty} (k_n/n!) x^n$. So for f, the Borel transform is given by

$$f_B(x) = \sum_{n=0}^{\infty} (-1)^n x^n = \frac{1}{1+x} \tag{2.41}$$

which converges for $|x| < 1$. The Borel resummation of f is then defined as $\tilde{f}$ by

$$\tilde{f}(x) = \int_0^{\infty} dz e^{-z} f_B(xz) \tag{2.42}$$

The integration has been shown in [10] to give the function $(e^{1/x}/x)\ \Gamma(0, 1/x)$ where $\Gamma(0, x)$ is the incomplete Gamma function, and this is well defined for all positive x. But near 0, the Taylor expansion of this resummed function matches exactly with the original function.Thus the Borel resummed function when compared with any finite order truncation of the original divergent series, gives the most sensible result. This is also observed in the case of diffusion and hydrodynamics, where a resummed expansion gives a more sensible result compared to finite order theories.

In [6], the Borel resummed theory is further shown to produce the exact fluctuations (2.28) as found in MIS theories. The hydrodynamic expansion (2.27) is Borel transformed, and is then analytically continued by the numerical method of Padé approximants. Integrating the Borel transform is shown to produce contour dependent ambiguities because of branch cut singularities. These however exactly agree with the fluctuations around the attractor solution (2.26), indicating how the MIS theory can be thought of as the resummed version of hydrodynamics. Further details on this resummation can be found in [6].

Chapter 3

Semi-holographically coupled systems

We have tried to model QGP dynamics in the hydrodynamic regime as a strongly interacting fluid in chapter 2. However some results from the Relativistic Heavy Ion Collider (RHIC) suggests the presence of some weakly coupled modes also in the QGP [7]. Before the onset of the hydrodynamic regime and immediately after it during hadronisation, weak couplings are expected to be present and can be modelled by a kinetic theory description. So a more effective approach would be to try coupling both strong and weakly interacting modes in a single system. However there is some difficulty to achieve this since the strongly interacting sector is usually modelled by a $\mathcal{N} = 4$ SYM fluid, while the weakly interacting sector is modelled by kinetic theory.

A recent approach developed to achieve this goal in [7, 8], is using couplings between effective metrics in the framework of semi-holography. This gives a very useful tool to couple two separate sectors with possibly different underlying theories and develop an effective theory of the collective system. The two separate sectors are assumed to behave like a fluid or kinetic theory and live in some different effective metric backgrounds which are created as a result of the interaction with the opposite sector. In this simplified model, this is the only way we assume the two sectors interact.

Coupling equations for these effective backgrounds are then written down such that conservation laws are obeyed by each sector, but morover, allowing the construction of a single conserved stress tensor for the collective system in the real physical background metric. Thus this gives a remarkably simple model to couple to two weakly or strongly interacting

sectors to give exciting results and a qualitative picture of the theory. This approach is explained in detail in the next section.

3.1 Coupling the effective metrics

We consider two subsystems $\mathcal{S}_1$, $\mathcal{S}_2$ of a larger collective system $\mathcal{S}$ living in a physical background metric $g^{(B)}_{\mu\nu}$. But the subsystems $\mathcal{S}_1$, $\mathcal{S}_2$ are assumed to live in some effective metrics $g^{\mu\nu}$, $\tilde{g}^{\mu\nu}$ respectively. We assume that these metrics are not physical metrics, but what the subsystem in its effective field theory description feels due to the interaction with the opposite system. So these are the only places where the interactions between the two sectors enter into the description. More explicitly, if $t^{\mu\nu}$, $\tilde{t}^{\mu\nu}$ are the effective stress tensors corresponding to $\mathcal{S}_1$, $\mathcal{S}_2$ respectively, then we assume $g^{\mu\nu} = g^{\mu\nu}(\tilde{t}^{\mu\nu}, ..)$, and $\tilde{g}^{\mu\nu} = \tilde{g}^{\mu\nu}(t^{\mu\nu}, ..)$. This is called a democratic coupling and is a simplified toy model to study coupled systems [7, 8].

So the interaction between sectors is determined by the coupling between the effective metrics. To form a reasonable theory, we require that

$$\nabla_\mu t^{\mu\nu} = 0, \quad \tilde{\nabla}_\mu \tilde{t}^{\mu\nu} = 0 \tag{3.1}$$

where ∇, $\tilde{\nabla}$ are the covariant derivatives in the effective metrics $g^{\mu\nu}$, $\tilde{g}^{\mu\nu}$ respectively. All raising and lowering of indices for any tensor associated with a subsector is assumed to be done by the individual effective metrics. We constrain the coupling equations so that there exists a $T^{\mu\nu}$ for the collective system living in the physical background $g^{(B)}_{\mu\nu}$, which satisfies

$$\nabla^{(B)}_\mu T^{\mu\nu} = 0 \tag{3.2}$$

where $\nabla^{(B)}$ is the covariant derivative for $g^{(B)}_{\mu\nu}$.

From the ward identity of the first subsystem $\nabla_\mu t^{\mu\nu} = 0$, using the relation $\Gamma^\mu_{\mu\rho} = \partial_\nu(ln\sqrt{-g})$, and multiplying by $\sqrt{-g}$, we get,

$$\partial_\mu(t^\mu_\nu\sqrt{-g}) - \frac{1}{2}t^{\mu\rho}\sqrt{-g}\partial_\nu g_{\mu\rho} = 0 \tag{3.3}$$

Using (3.3) and its analogue for the second system, it is possible to show that for the following coulping equations between the effective metrics and the background, we can construct a total conserved $T^{\mu\nu}$ for the whole system [7].

$$g_{\mu\nu} = g^{(B)}_{\mu\nu} + \left(\gamma g^{(B)}_{\mu\rho}\tilde{t}^{\rho\sigma}g^{(B)}_{\sigma\nu} + \gamma' g^{(B)}_{\mu\nu}g^{(B)}_{\rho\sigma}\tilde{t}^{\rho\sigma}\right)\frac{\sqrt{-\tilde{g}}}{\sqrt{-g^{(B)}}} \tag{3.4}$$

$$\tilde{g}_{\mu\nu} = g^{(B)}_{\mu\nu} + \left(\gamma g^{(B)}_{\mu\rho}t^{\rho\sigma}g^{(B)}_{\sigma\nu} + \gamma' g^{(B)}_{\mu\nu}g^{(B)}_{\rho\sigma}t^{\rho\sigma}\right)\frac{\sqrt{-g}}{\sqrt{-g^{(B)}}} \tag{3.5}$$

Here γ, γ' are coupling constants which determine the strength of coupling between the two sectors.

To construct the explicit form of $T^{\mu\nu}$, we can note that for

$$\begin{aligned}\Delta K = &-\frac{\gamma}{2}\left(t^{\mu\rho}\frac{\sqrt{-g}}{\sqrt{-g^{(B)}}}\right)g^{(B)}_{\rho\sigma}\left(\tilde{t}^{\sigma\nu}\frac{\sqrt{-\tilde{g}}}{\sqrt{-g^{(B)}}}\right)g^{(B)}_{\nu\mu}\\ &-\frac{\gamma'}{2}\left(t^{\mu\nu}\frac{\sqrt{-g}}{\sqrt{-g^{(B)}}}\right)g^{(B)}_{\mu\nu}\left(\tilde{t}^{\rho\sigma}\frac{\sqrt{-\tilde{g}}}{\sqrt{-g^{(B)}}}\right)g^{(B)}_{\rho\sigma}\end{aligned}$$

using (3.3), for $K^{\mu}{}_{\nu}$, $L_{\mu}{}^{\nu}$ defined below, $\nabla_\mu K^{\mu}{}_{\nu} = 0$, and $\nabla_\nu L_{\mu}{}^{\nu} = 0$ [7].

$$K^{\mu}{}_{\nu} = t^{\mu}{}_{\nu}\sqrt{-g} + \tilde{t}^{\mu}{}_{\nu}\sqrt{-\tilde{g}} + \Delta K\delta^{\mu}{}_{\nu} \tag{3.6}$$

$$L_{\mu}{}^{\nu} = t_{\mu}{}^{\nu}\sqrt{-g} + \tilde{t}_{\mu}{}^{\nu}\sqrt{-\tilde{g}} + \Delta K\delta_{\mu}{}^{\nu} \tag{3.7}$$

So a symmetric second rank tensor $T^{\mu\nu}$ obeying $\nabla_\mu T^{\mu\nu} = 0$ can be defined as

$$T^{\mu}{}_{\nu} = \frac{1}{2}(K^{\mu}{}_{\nu} + L_{\nu}{}^{\mu}) \tag{3.8}$$

This will be used as the effective stress tensor for the combined system in the physical background $g^{(B)}_{\mu\nu}$.

3.2 Coupled ideal fluids

To study the consequences of this form of coupling between two systems, the first attempt is to consider two fluids which are very close to equilibrium and can be approximated by zeroth order hydrodynamics [7]. This can later be generalised to MIS fluids or kinetic theory to model QGP. But even though this is a very simple scenario, we get a lot of qualitative intuition regarding the dynamics of the total system and also encounter an exciting phase transition in the combined system.

We consider the total system to be living in the Minkowski background $\eta_{\mu\nu}$ and consider the scenario where both the sectors have had sufficient time to interact with each other and reach a near equilibrium state defined by subsystem temperatures T_1 and T_2. This allows us to expect the total system also to be close to an equilibrium defined by some temperature T. We can then use zeroth order hydrodynamics

$$T^{\mu\nu} = (\varepsilon + P)U^\mu U^\nu + P\eta^{\mu\nu} \tag{3.9}$$

with U^μ = (1,0,0,0) the fluid velocity, ε the energy density, and P the pressure of the whole system.

Similarly for the subsystems we have

$$t^{\mu\nu} = (\epsilon_1(T_1) + P_1(T_1))u^\mu u^\nu + P_1(T_1)g^{\mu\nu}, \quad \tilde{t}^{\mu\nu} = (\epsilon_2(T_2) + P_2(T_2))\tilde{u}^\mu \tilde{u}^\nu + P_2(T_2)\tilde{g}^{\mu\nu} \tag{3.10}$$

where $\epsilon_1, \epsilon_2, P_1, P_2, T_1, T_2$ are the individual energy densities, pressures, and temperatures. We continue to work with conformal fluids and so

$$\epsilon_1(T_1) = 3n_1T_1^4, \quad P_1(T_1) = n_1T_1^4, \quad \epsilon_2(T_2) = 3n_2T_2^4, \quad P_2(T_2) = n_2T_2^4 \tag{3.11}$$

n_1, n_2 are some constants depending on the underlying theory.

The effective metrics can be assumed to be stationary, but they may not be flat in the presence of the interaction between the subsystems. But from symmetry considerations we can assume the following forms [7]

$$g_{\mu\nu} = diag(-a^2, b^2, b^2, b^2), \quad \tilde{g}_{\mu\nu} = diag(-\tilde{a}^2, \tilde{b}^2, \tilde{b}^2, \tilde{b}^2). \tag{3.12}$$

So the individual normalised fluid velocities would be $u^\mu = (1/a, 0, 0, 0)$, $\tilde{u}^\mu = (1/\tilde{a}, 0, 0, 0)$.

The total energy momentum can be computed from (3.8), and comparison with (3.9) gives the energy density and pressure of the combined fluid.

$$\varepsilon = \epsilon_1(T_1)ab^3 + \epsilon_2(T_2)\tilde{a}\tilde{b}^3 + \frac{\gamma}{2}\left(\frac{\epsilon_1(T_1)\epsilon_2(T_2)}{a^2\tilde{a}^2} + \frac{3P_1(T_1)P_2(T_2)}{b^2\tilde{b}^2}\right)ab^3\tilde{a}\tilde{b}^3 + \frac{\gamma'}{2}\left(-\frac{\epsilon_1(T_1)}{a^2} + \frac{3P_1(T_1)}{b^2}\right)\left(-\frac{\epsilon_2(T_2)}{\tilde{a}^2} + \frac{3P_2(T_2)}{\tilde{b}^2}\right)ab^3\tilde{a}\tilde{b}^3$$

$$P = P_1(T_1)ab^3 + P_2(T_2)\tilde{a}\tilde{b}^3 - \frac{\gamma}{2}\left(\frac{\epsilon_1(T_1)\epsilon_2(T_2)}{a^2\tilde{a}^2} + \frac{3P_1(T_1)P_2(T_2)}{b^2\tilde{b}^2}\right)ab^3\tilde{a}\tilde{b}^3 - \frac{\gamma'}{2}\left(-\frac{\epsilon_1(T_1)}{a^2} + \frac{3P_1(T_1)}{b^2}\right)\left(-\frac{\epsilon_2(T_2)}{\tilde{a}^2} + \frac{3P_2(T_2)}{\tilde{b}^2}\right)ab^3\tilde{a}\tilde{b}^3$$

To find the relation between the subsystem temperatures and the total temperature, we can think of T as defined through the imaginary time formalism by $1/T = \int_0^\beta d\tau$, where τ is the imaginary time with period β [7]. For the subsystems which live in $g_{\mu\nu}, \tilde{g}_{\mu\nu}$, similarly

$$T_1^{-1} = \int_0^\beta \sqrt{-g_{00}}d\tau = a\beta, \quad T_2^{-1} = \int_0^\beta \sqrt{-\tilde{g}_{00}}d\tau = \tilde{a}\beta \tag{3.13}$$

This gives the subsystem temperatures as $T_1 = T/a$, $T_2 = T/\tilde{a}$.

For the subsystems, the respective light-cone velocities $v, \tilde{v}$ are defined as

$$v = \frac{a}{b}, \quad \tilde{v} = \frac{\tilde{a}}{\tilde{b}} \tag{3.14}$$

Also defining the ratio $-\gamma'/\gamma = r$, the metric coupling equations (3.4), (3.5) give

$$1 - v^2b^2 = 3\gamma T^4 n_2 \frac{1 - r(1 - \tilde{v}^2)}{\tilde{v}^5\tilde{b}^2} \tag{3.15}$$

$$1 - \tilde{v}^2\tilde{b}^2 = 3\gamma T^4 n_1 \frac{1 - r(1 - v^2)}{v^5b^2} \tag{3.16}$$

$$b^2 - 1 = \gamma T^4 n_2 \frac{\tilde{v}^2 + 3r(1 - \tilde{v}^2)}{\tilde{v}^5\tilde{b}^2} \tag{3.17}$$

$$\tilde{b}^2 - 1 = \gamma T^4 n_1 \frac{v^2 + 3r(1-v^2)}{v^5 b^2} \tag{3.18}$$

There are certain restrictions on the metric coupling coefficients to ensure causality is not violated. Adding (3.15) and (3.17) gives $(1-v^2) > 0$ only if $\gamma > 0$, and similarly from (3.16) and (3.18), $(1-\tilde{v}^2) > 0$ only if $\gamma > 0$. So this restriction on γ has to be maintained to keep the theory causal.

By eliminating $\tilde{b}$ from (3.16) and (3.18) we get

$$n_1 \gamma T^4 = \frac{v^5(1-\tilde{v}^2)(3+\tilde{v}^2)}{(3+v^2\tilde{v}^2 - 3r(1-v^2)(1-\tilde{v}^2))^2} \tag{3.19}$$

And by eliminating b from (3.15) and (3.17) we get

$$n_2 \gamma T^4 = \frac{\tilde{v}^5(1-v^2)(3+v^2)}{(3+v^2\tilde{v}^2 - 3r(1-v^2)(1-\tilde{v}^2))^2} \tag{3.20}$$

The denominators of these equations which are identical, can stay non-negative but attain zero, only if $r > 1$. This condition is needed so that the temperature T is not restricted to some finite value. So when $r > 1$, the theory is UV complete as the temperature can go to infinity [7]. Hence we impose this restriction on possible values r can take.

As usual, the entropy density S for the whole system and s_1, s_2 respectively for the subsystems are defined thermodynamically by

$$\epsilon_1 + P_1 = T_1 s_1, \quad \epsilon_2 + P_2 = T_2 s_2, \quad \varepsilon + P = TS \tag{3.21}$$

Using the relations for the subsystem energy and pressure (3.11), the subsystem temperatures T_1 and T_2 (3.13), the light-cone velocities (3.14), and the constitutive relations for the total energy density and pressure,

$$S = 4T^3 \left(\frac{n_1}{v^3} + \frac{n_2}{\tilde{v}^3} \right) \tag{3.22}$$

This relation is useful later in computing the thermodynamic sound speed c_s in the system

$$c_s^2 = \frac{dP}{d\varepsilon} = \left(\frac{d\,lnS}{d\,lnT} \right)^{-1} \tag{3.23}$$

The total system can now be numerically solved for any values of n_1, n_2. Any variable in

the theory is a function of only the system temperature T since we are studying the theory near an equilibrium solution characterised uniquely by this T. The coupling equations (3.15) to (3.18) can give $a, \tilde{a}, b, \tilde{b}$ as functions of the two light-cone velocities $v, \tilde{v}$. But (3.19), (3.20) can be numerically solved to get $v, \tilde{v}$ as functions of T alone. So all other functions like the total energy density or pressure can be numerically solved as a function of T. The conservation equations are by definition always satisfied for the total stress tensor in (3.9).

3.3 The second order phase transition

When solving the system as mentioned earlier, we encounter a second-order phase transition with a critical point [7]. This is easiest to see in the case of identical subsystems when $n_1 = n_2 = n$, which also requires $v = \tilde{v}$ and so $a = \tilde{a}$, and $b = \tilde{b}$ from the symmetry of the coupling equations (3.17) and (3.18). In this simplified case (3.19) and (3.20) identically give γT^4 as an analytic function of v.

$$n\gamma T^4 = \frac{v^5(1-v^2)(3+v^2)}{(3+v^4-3r(1-v^2)^2)^2} \tag{3.24}$$

This is plotted in Fig. 3.1 to see a phase transition with a critical point as the paramater r is varied for $r > 1$, as originally shown in [7]. As r is varied from 1 to higher values, we see a critical point at an intermediate value $r = r_c$ where the curve transitions from having two extrema to just having one point of inflection at $v = v_c$. As seen later, this leads to the second derivative of v as a function of $\gamma^{1/4}T$ blowing up at r_c. This shows why the phase transition is second order at r_c, as the first derivative of v as a function of T is discontinuous at r_c while the function itself is continuous. But as will be explained later in this section when studying the total entropy of the system, the phase transition is first order below r_c with a discontinuity in the function indicative of superheating and supercooling. The critical point is determined analytically by finding the v_c which extremises the function $r(v)$ obtained in turn by extremising $n\gamma T^4(v)$ and its v derivative at the inflection point. This critical point is easily computed in appendix D. of [7] to be at $v_c \sim 0.35097$, $r_c \sim 1.114509$, and $n\gamma T_c^4(v) \sim 0.0539768$.

When plotting these curves, we initially also encounter an additional branch of solution. But these are found to be unphysical since they do not behave as required in the decoupling

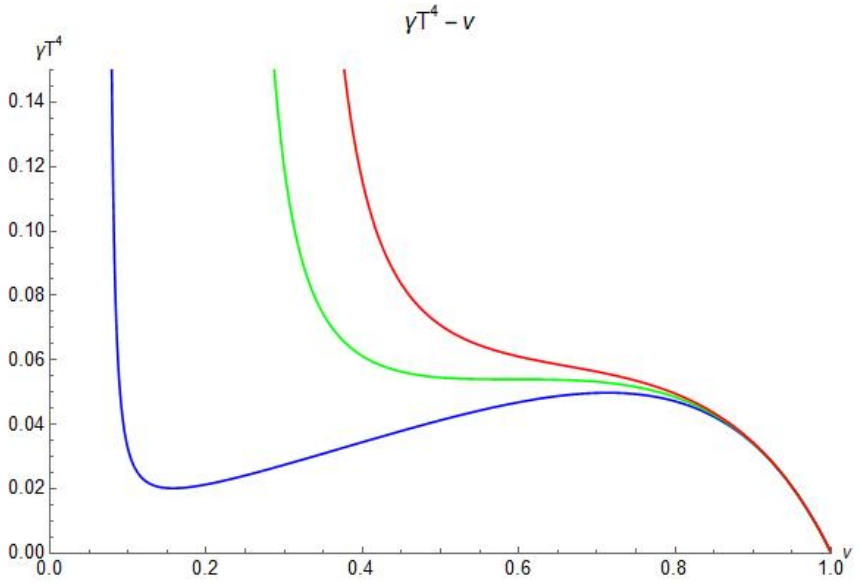

Figure 3.1: $\gamma T^4 - v$ *for coupled identical ideal fluids.* The blue, green, and red curves are the analytical solutions for γT^4 as a function of v for $r = 1.0, r = 1.11451$, and $r = 1.2$ respectively. The critical point occurs for $r = r_c \sim 1.11451$.

limit , i.e., when $\gamma \to 0$. In this limit, we expect the two fluids to completely decouple with no interactions between them, and so the individual effective metrics should go to the Minkowski metric, taking the light-cone velocities to one. This indeed occurs in the physical branch plotted at each r, but does not happen in the unphysical branches. This is shown in Fig. 3.2. The presence of an unphysical branch is something which recurs for all curves plotted later, but in each case, the behaviour as $\gamma \to 0$ distinguishes it from the physical branch.

It has also been shown in [7] that $|\gamma T^4 - \gamma T_c^4| \sim |v - v_c|^3$ near the critical point (Similar results are derived for the entropy and diffusion constant below). This relation allows for the computation of the critical exponent α for the specific heat C_V since $C_V = T\partial S/\partial T$, and near the critical point, we expect

$$|S - S_c| \sim 24 n T_c^3 v_c^{-4} |v - v_c| \tag{3.25}$$

where we have used the form of S in (3.22) and used the assumption that the two fluids are identical. And since $|T^4 - T_c^4| \sim 4T_c^3 |T - T_c|$, we get

$$|S - S_c| \sim |T - T_c|^{1/3} \tag{3.26}$$

This easily shows that the critical exponent α is 2/3 for C_V. The scaling behaviour of the entropy is explicitly solved later to show the validity of this derivation in Fig. 3.8.

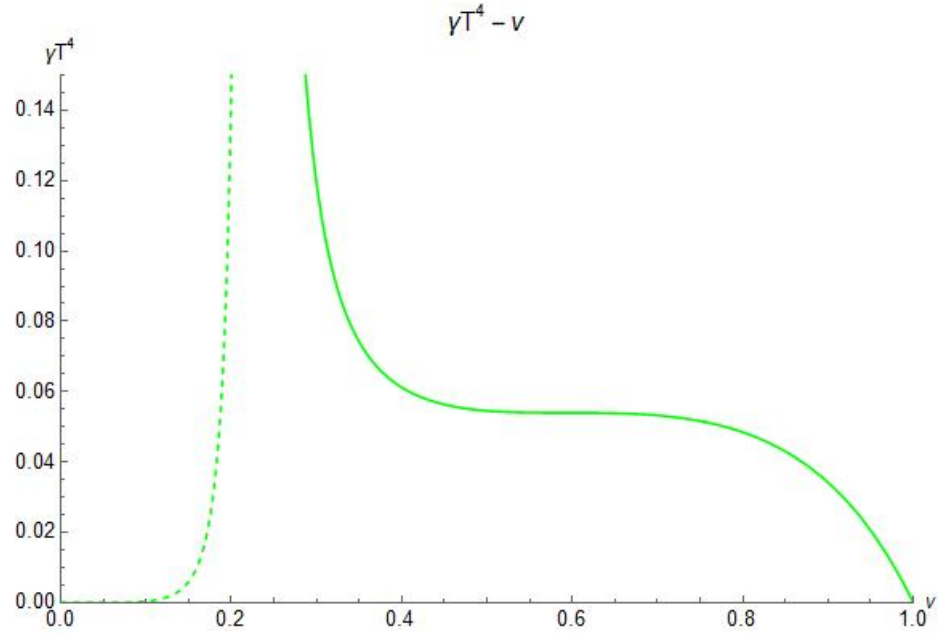

Figure 3.2: *Physical and unphysical branches in the $\gamma T^4 - v$ plot.* The dotted line represents the unphysical branch for a particular r (here r_c) while the solid curve is the physical branch. Only the solid curve goes to $v = 1$ at $\gamma T^4 = 0$.

The relation $\gamma T^4(v)$ can be inverted numerically to plot v as a function of γT^4 [7] (we take $n = 1$ for simplicity) as reproduced in Fig. 3.3. The system encounters a second-order phase transition at r_c, where though the function v is continuous, the first derivative blows up at T_c. Below r_c, the solution is multivalued which indicates a first order phase transition due to supercooling and superheating phases (explained later when discussing entropy in this section). The region denoted by the dotted lines in the blue curve in Fig. 3.3 is unphysical which will also be clear after studying the entropy curve. For all values above r_c there exists a well-defined and smooth curve for v.

Since v can be numerically solved as a function of γT^4, the coupling equations (3.15 - 3.18) can be written as analytic expressions in v and γT^4, and then numerically solved as a

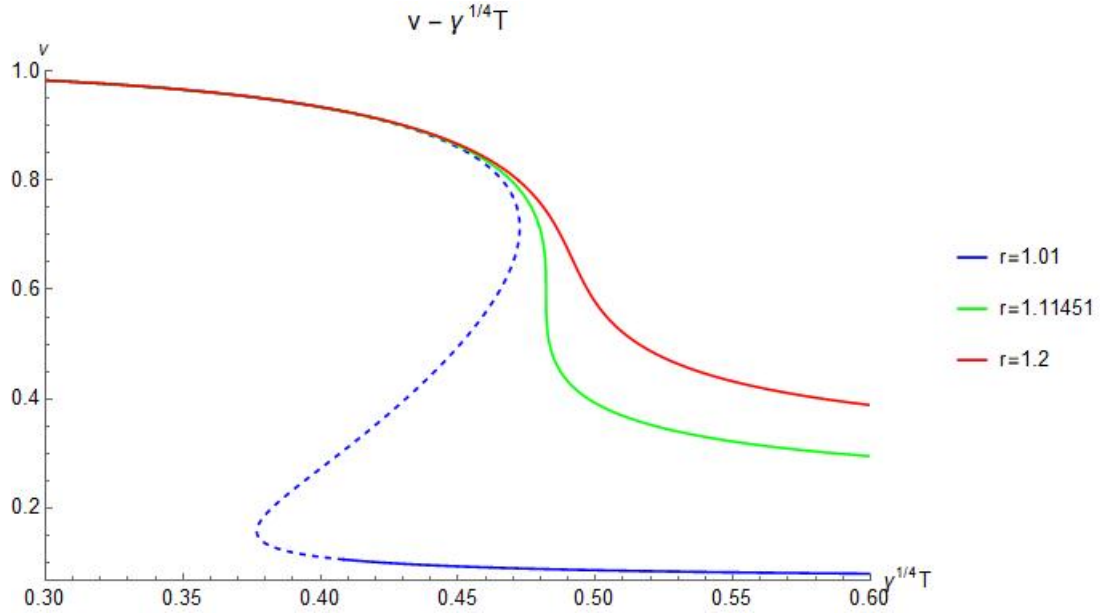

Figure 3.3: *Numerical solution of* v. The dotted part of the blue curve is unphysical. A jump happens between the solid blue curves below r_c due to superheating or supercooling. The green curve has a blow up of its derivative at T_c. The red curve is smooth.

function of γT^4 alone. b^2 has the analytic form

$$b_1^2 = -\frac{\sqrt{4\gamma_1 T^4 v^7 \left(v^2 - 3r\left(v^2-1\right)\right) + \left(\gamma_1 T^4 \left(3r\left(v^2-1\right)^2 - v^4 - 3\right) + v^5\right)^2}}{2v^7} + \frac{3\gamma_1 r T^4 + 3\gamma_1 r T^4 v^4 - 6\gamma_1 r T^4 v^2 - 3\gamma_1 T^4 - \gamma_1 T^4 v^4 + v^5}{2v^7}$$

and a^2 similarly has the analytic solution which is computed using $a = vb$.

The numerical solutions are derived in Fig. 3.4 for b, and Fig. 3.5 for a. We see the critical behaviour of both functions at r_c where the first derivative blows up for b, and becomes discontinuous for a. Below r_c the functions show a first order crossover, and above r_c they are smooth single-valued functions.

These solutions computed here can also be verified by computing the individual subsystem temperatures T/a as functions of $\gamma^{1/4}T$. This is verified to be in exact agreement with [7] and is shown in Fig. 3.6. The first derivative is discontinuous for r_c, while multiple solutions exist below r_c showing a first order transition. We can also similarly reproduce all the identical system curves produced in [7].

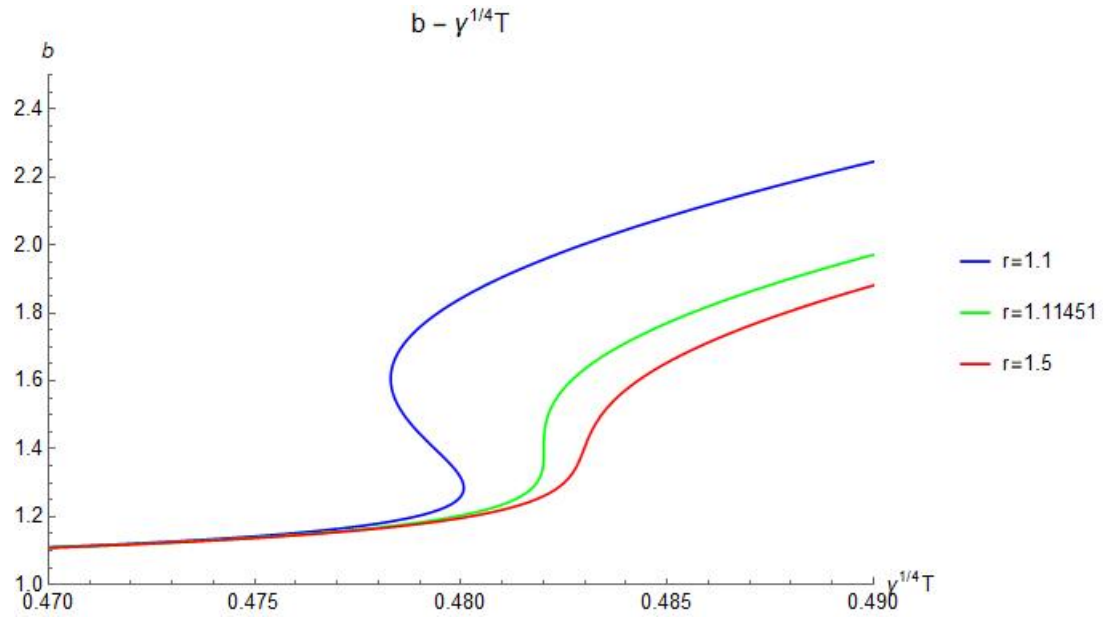

Figure 3.4: *Numerical solution of b.* The green curve has its first derivative blow up at T_c. Crossover occurs for the blue curve.

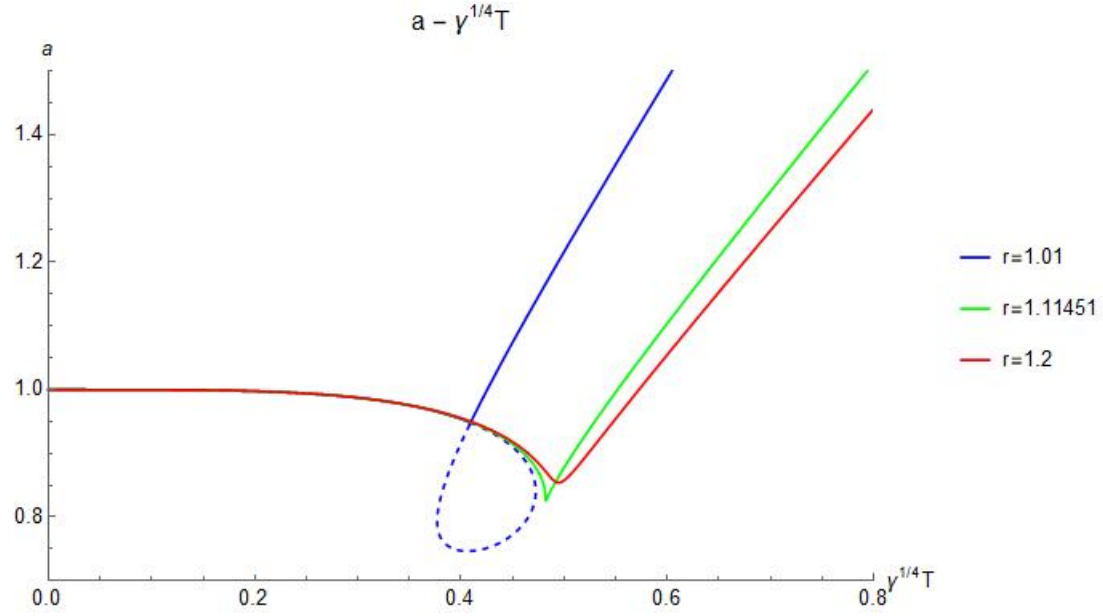

Figure 3.5: *Numerical solution of a.* The slope of the green curve is discontinuous at T_c. Crossover occurs in the blue curve.

We are interested in studying the evolution of the total entropy of the system defined in (3.22). This would help us understand physically the crossover and the critical point. The dimensionless quantity S/T^3 is derived below in Fig. 3.7.

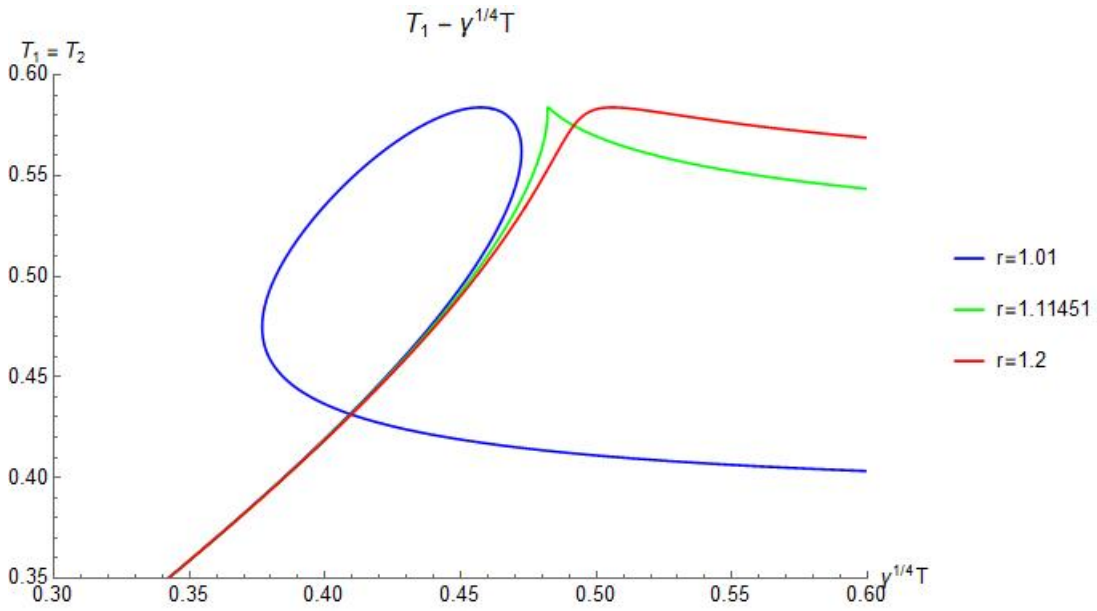

Figure 3.6: *Subsystem temperature as a function of the total temperature.* $T_1 = T_2$ also shows critical behaviour at $r_c \sim 1.11451$, and crossover below r_c.

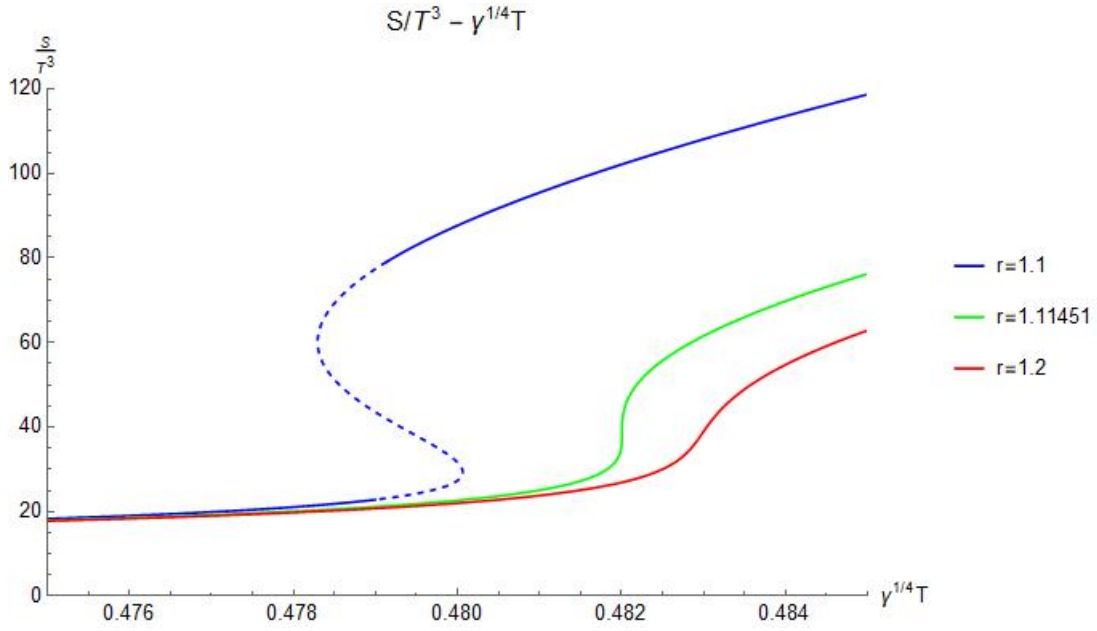

Figure 3.7: *Total entropy curve.* Critical point occurs for r_c (green curve), while crossover occur below it. The dotted blue lines correspond to the superheating and supercooling phases.

In the entropy curve, below r_c, i.e. for the blue curve in Fig. 3.7, the continuous dotted

curve which connects the two endpoints of the solid curves is an unphysical region since here the entropy seems to have a negative slope which is unphysical. So the system undergoes superheating when approaching the dicontinuity from lower temperatures by a sudden jump in the entropy. Supercooling occurs when this jump is approached from a higher temperature. This kind of a jump is exactly what happens for all other variables below r_c. They exhibit supercooling or superheating depending on how the entropy is affected at the jump.

Since v has a critical behaviour $|v - v_c| \sim |T - T_c|^{1/3}$, we expect all analytic functions of v to exhibit a similar scaling behaviour close to T_c. This is explicitly checked to be true for the total entropy S by computing the logarithmic plot of $|S - S_c|$ near the critical point in Fig. 3.8. We get a straight curve whose slope is very close to 1/3 (we do not get extremely accurate results because of the loss of precision in plotting the points even when using very precise values of r_c, v_c, and T_c. Numerically getting a large number of points very close to T_c is also difficult, and so the log plot has to be extrapolated). This is also later verified for the diffusion constant in the next section.

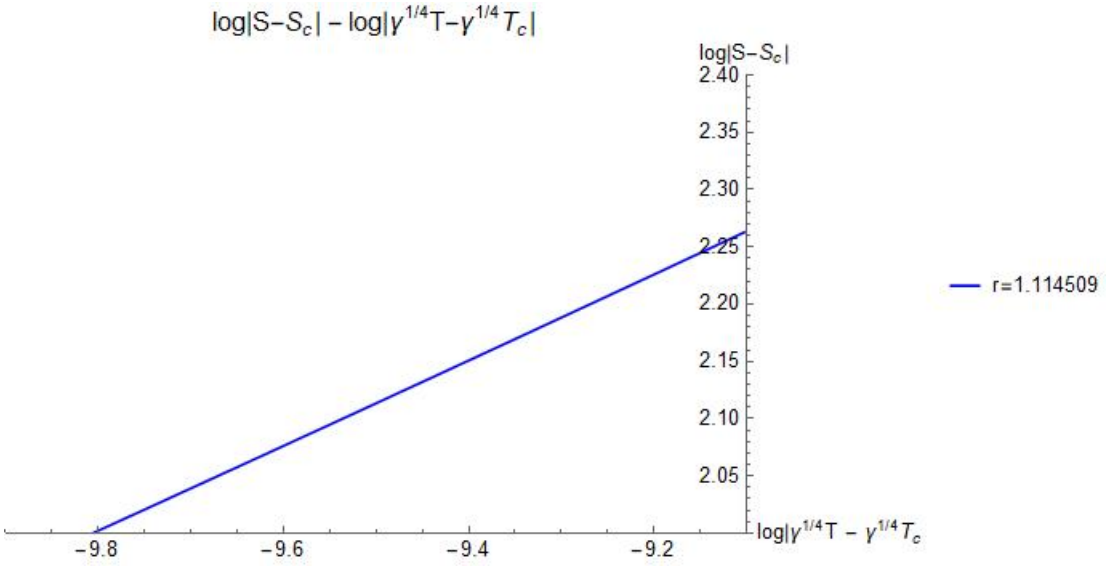

Figure 3.8: *Logarithmic plot of S near the critical point.* The slope of the curve is seen to be $\sim (2.26 - 2.0)/(9.8 - 9.1) \sim 0.37$, close to 1/3.

Another important physical quantity whose critical behaviour we are interested in is the thermodynamic speed of sound c_s defined in (3.23). This speed is numerically computed below in Fig. 3.9 to show that it not only has a crtical point at $r = r_c$ (due to the discontinuity in the slope), but it also vanishes exactly at this point. This is a remarkable result which

confirms our expectation that at the critical point, due to the existence of correlations at all length scales, there should not be any thermodynamic propagation. For any other value of r_c, there is no critical point and the sound speed does not drop to zero. In the decoupling limit when $\gamma \to 0$, we get the expected conformal sound speed in four dimensions, $1/\sqrt{3}$.

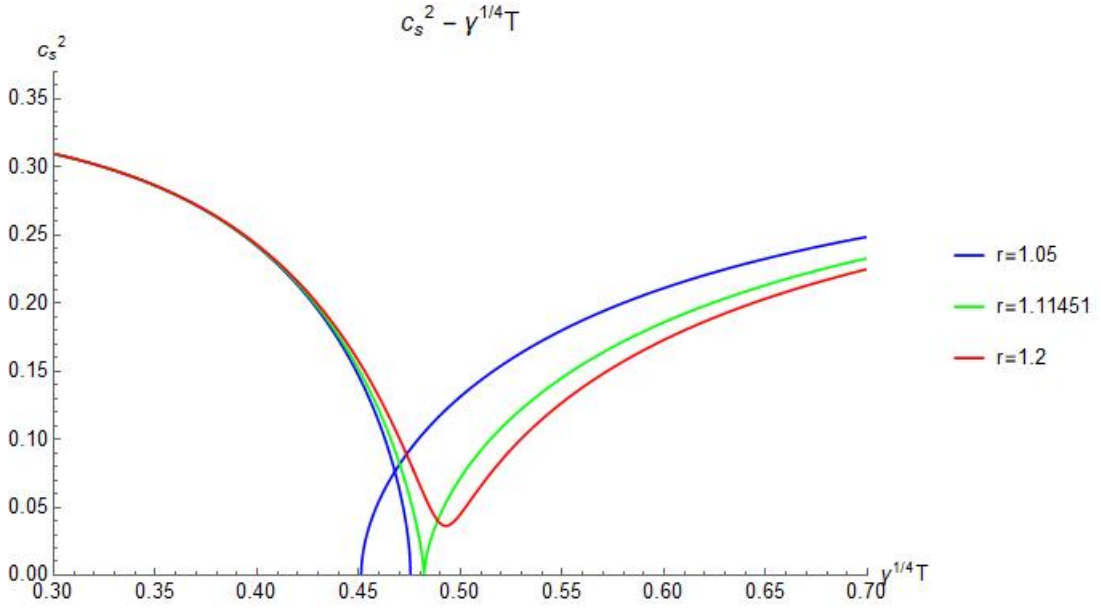

Figure 3.9: *Thermodynamic sound speed solutions* The thermodynamic sound speed vanishes exactly at the critical point when $r = r_c$ (green curve).

We would also like to compute the dispersion relation for a sound like perturbation to the coupled system and find the critical behaviour for the sound speeds in such modes. It is very useful to study the behaviour of all the different hydrodynamic modes in this case of two coupled ideal fluids. This allows us to further study the sound speed in the sound channel, and see the presence of attenuation in these modes. Their critical behaviour is calculated in section 3.5. Such calculations can also be done in the shear sector to compute the diffusion constant in the shear modes, and study their critical behaviour (section 3.4). Moving to two coupled MIS fluids allows us to study non-hydrodynamic modes for the first time in coupled systems.

3.4 Diffusion constant in Shear sector

To compute the shear modes, similar to the case of a single fluid, we assume the combined system and the subsystems are close to equilibrium. We then assume fluctuations which lie in the shear sector (section 2.7) for the hydrodynamic fields, and treat the modified system with the fluctuations as obeying first order hydrodynamics [7].

Due to rotational symmetry (as Boost invariance is broken by the equilibrium), we can assume the propagation of fluctuations to be in the z-direction. But characteristic of the shear sector, the velocity fields will be perpendicular to the propagation direction, and is assumed to be along x. To retain the normalisation, these will have the form

$$u^\mu = (\frac{1}{a}, \nu, 0, 0), \quad \tilde{u}^\mu = (\frac{1}{\tilde{a}}, \tilde{\nu}, 0, 0) \tag{3.27}$$

where the perturbations $\nu, \tilde{\nu}$ can be assumed to have a propagating wave like form $\sim e^{i(kz-\omega t)}$. Such a form can also be assumed for any other perturbation in the system.

The effective metrics also have perturbations which couple with each other through the coupling equations (3.15) - (3.18). Since the velocity flow is along x while the propagation vector is along z, in the shear sector, only the tx and xz components of the metrics have perturbations. The unperturbed metrics are the same as defined in (3.12). So

$$\delta g_{01} = \beta, \quad \delta g_{13} = \gamma_{13}, \quad \delta \tilde{g}_{01} = \tilde{\beta}, \quad \delta \tilde{g}_{13} = \tilde{\gamma}_{13} \tag{3.28}$$

The first order stress tensor can be expanded upto first order in these perturbations to find that it only invloves a modification to the ideal stress tensor by

$$\delta t^{01} = -\frac{P_1}{a^2 b^2}\beta + \frac{(P_1 + \epsilon_1)}{b}\nu, \quad \delta t^{13} = -\frac{P_1}{b^4}\gamma_{13} + \frac{\eta}{b^2}\partial_z \nu - \frac{\eta}{ab^4}\partial_t \gamma_{13} \tag{3.29}$$

$$\delta \tilde{t}^{01} = -\frac{P_2}{\tilde{a}^2 \tilde{b}^2}\tilde{\beta} + \frac{(P_2 + \epsilon_2)}{\tilde{b}}\tilde{\nu}, \quad \delta \tilde{t}^{13} = -\frac{P_2}{\tilde{b}^4}\tilde{\gamma}_{13} + \frac{\tilde{\eta}}{\tilde{b}^2}\partial_z \tilde{\nu} - \frac{\tilde{\eta}}{\tilde{a}\tilde{b}^4}\partial_t \tilde{\gamma}_{13} \tag{3.30}$$

where η and $\tilde{\eta}$ are the shear viscosity coefficients for the two subsystems.

The equations available to solve these perturbations to the system are the two ward identities (3.1) and the four coupling equations (3.15) - (3.18). These give the required six

equations in the perturbations ν, $\tilde{\nu}$, β, $\tilde{\beta}$, γ_{13}, and $\tilde{\gamma}_{13}$. Taking the Fourier transform of these equations, the four relations obtained from the coupling equations are solved to get the metric perturbations β, $\tilde{\beta}$, γ_{13}, and $\tilde{\gamma}_{13}$ as functions of ν, $\tilde{\nu}$. Substituting these back in the two ward identities gives a set of two homogenous equations in ν, and $\tilde{\nu}$. For the existence of a non-trivial solution for ν, and $\tilde{\nu}$, we need the determinant of the 2×2 coefficient matrix for the system of equations in ν, and $\tilde{\nu}$ to be zero. This gives the required equation in ω, k which has to be solved for the dispersion relation $\omega(k)$ [7]. At leading order, the behaviour is determined to be,

$$\omega(k) = -iDk^2 + \mathcal{O}(k^3) \tag{3.31}$$

So the leading behaviour is seen to be a diffusive mode with diffusion constant D which has two solutions. For identical fluids, they are computed here

$$D_1 = \frac{a^2\left(a^5 - b\gamma T^4\right)}{4\pi b^2 T\left(a^5 + 3b\gamma T^4\right)}, \quad D_2 = -\frac{a^2\left(a^5 + b\gamma T^4\right)}{4\pi b^2 T\left(3b\gamma T^4 - a^5\right)} \tag{3.32}$$

These two diffusion modes are numerically solved and plotted in Fig. 3.10, Fig. 3.11, and Fig. 3.12.

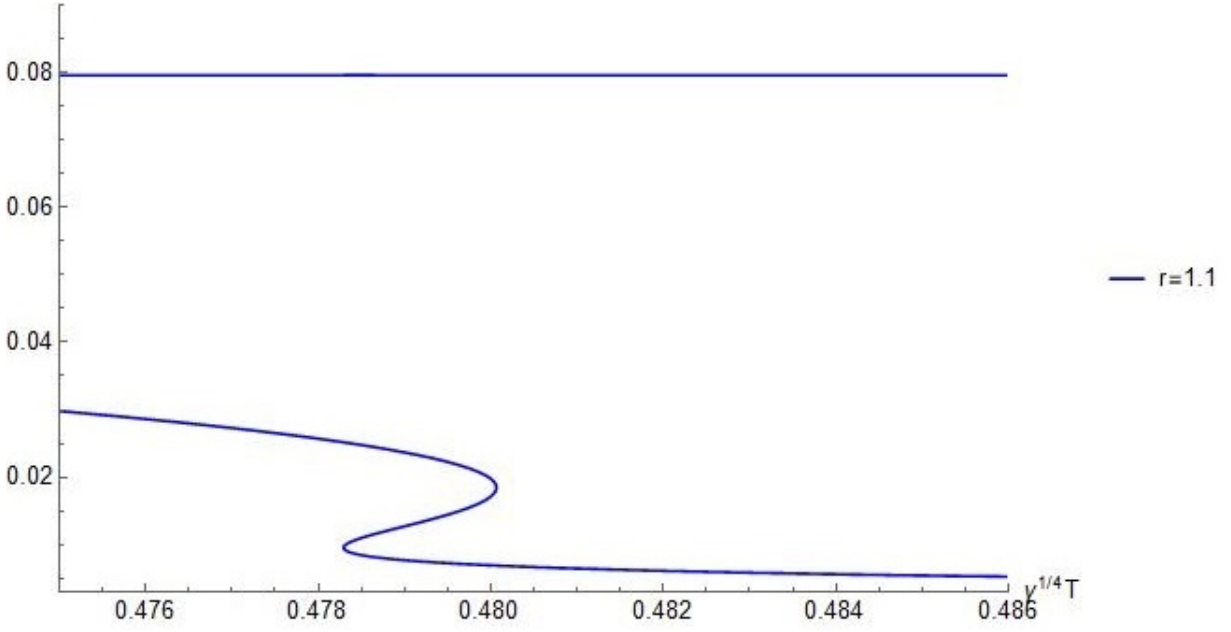

Figure 3.10: *The two diffusion modes below r_c.*

This is very useful in understanding the behaviour of the shear modes near the critical point. As before, we are able to observe a second order phase transition at $r = r_c$, where

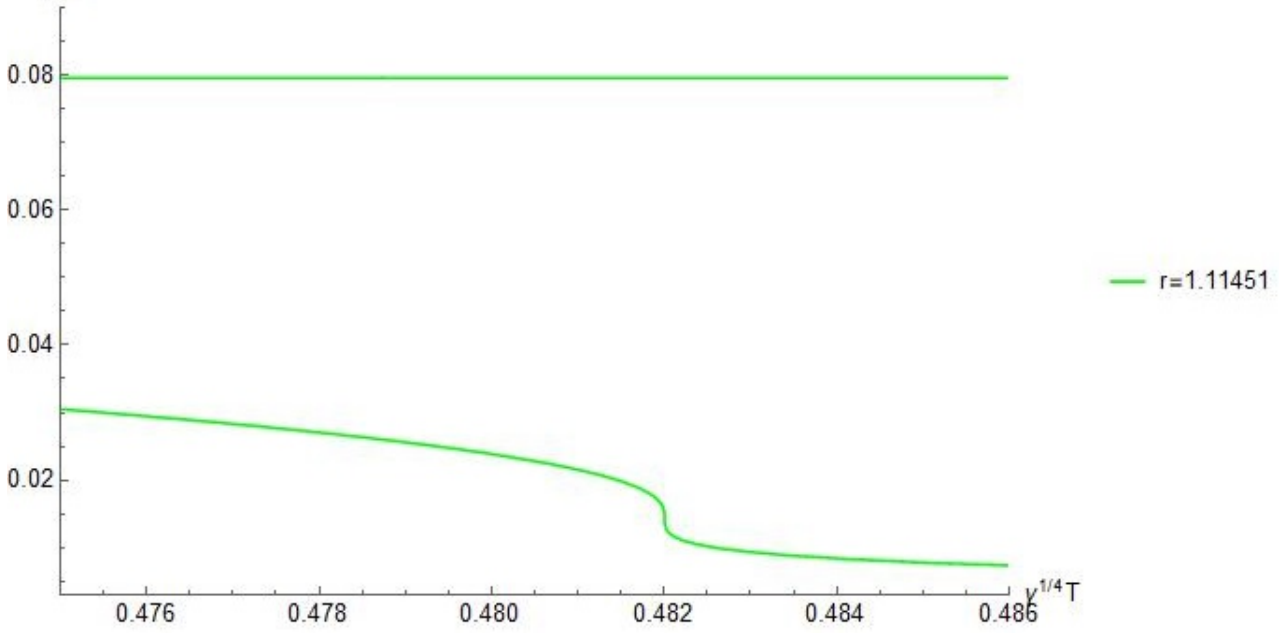

Figure 3.11: *The two diffusion modes at r_c.*

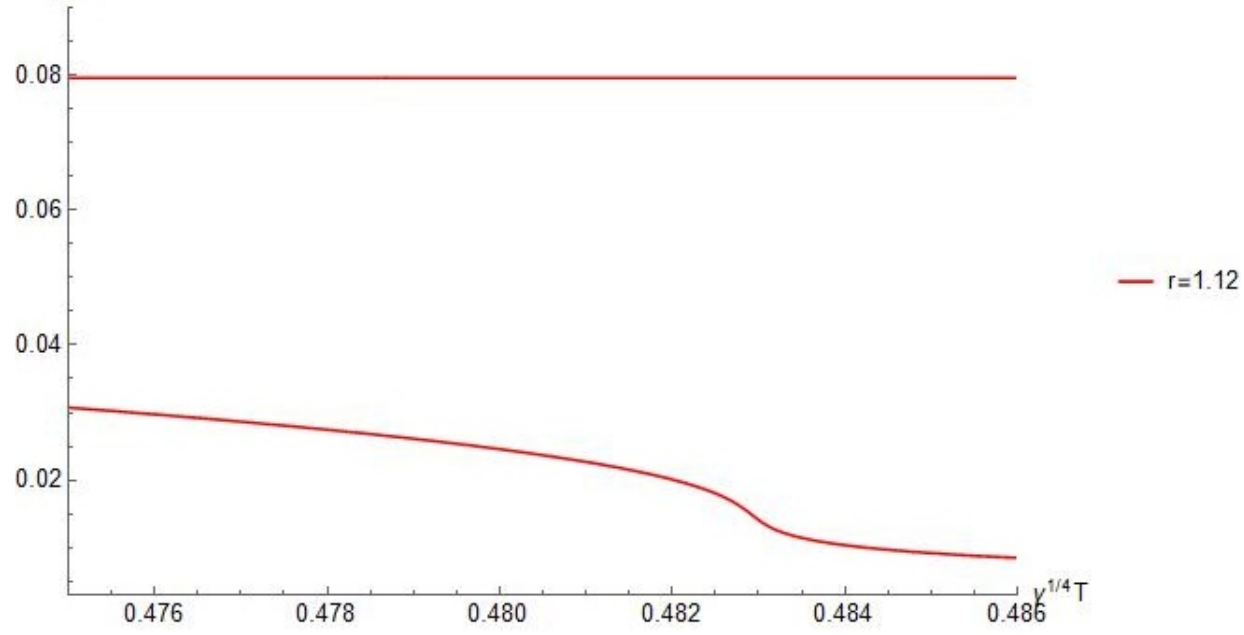

Figure 3.12: *The two diffusion modes above r_c.*

the derivative of the diffusion constant blows up for one of the modes. However the second mode remains constant for all r. But the diffusion constant clearly does not vanish at the critical point unlike the thermodynamic sound speed in Fig. 3.9. This indicates some non-

zero transport even at the critical point. A log-log plot of $|D - D_c|$ again confirms it is proportional to $|T - T_c|^{1/3}$ near T_c (Fig. 3.13).

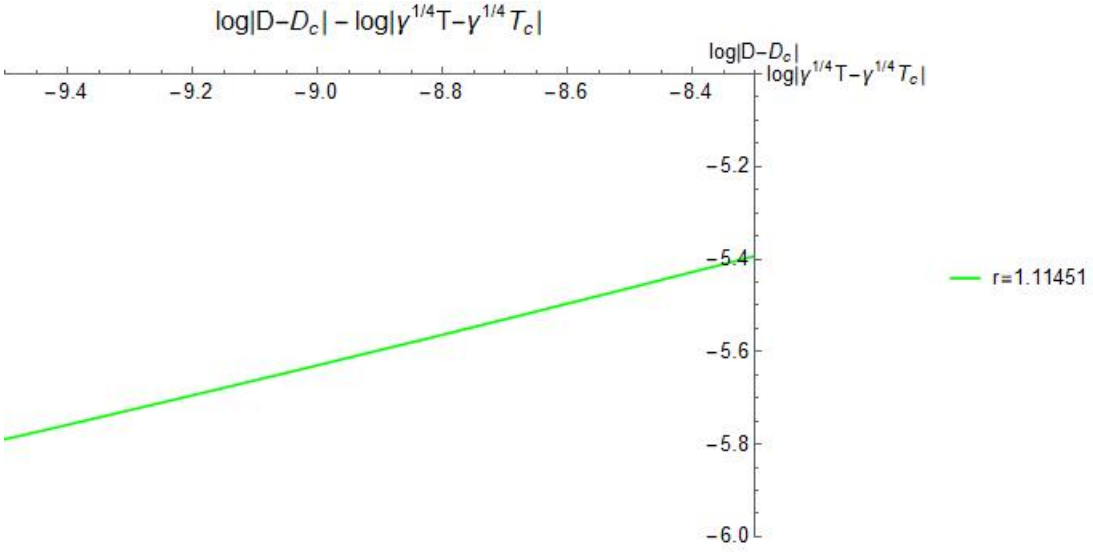

Figure 3.13: *Logarithmic plot of D near the critical point.* The slope of the line is $\sim (5.8 - 5.4)/(9.5 - 8.3) = 1/3$.

3.5 Sound speed and Attenuation in Sound sector

For the same system of two ideal coupled fluids, close to equilibrium for the total system and the individual subsystems, we choose propagation of fluctuations in the z-direction. However, characteristically for the sound sector the perturbations align along the same direction as the propagation direction. Hence the effective metrics have the form in (3.12) with the general form of perturbations permitted by symmetry given as

$$\delta g_{00} = -2a\delta a, \quad \delta g_{11} = \delta g_{22} = 2b\delta b + \chi, \quad \delta g_{33} = 2b\delta b - 2\chi, \quad \delta g_{03} = \beta \tag{3.33}$$

$$\delta \tilde{g}_{00} = -2\tilde{a}\delta\tilde{a}, \quad \delta \tilde{g}_{11} = \delta \tilde{g}_{22} = 2\tilde{b}\delta\tilde{b} + \tilde{\chi}, \quad \delta \tilde{g}_{33} = 2\tilde{b}\delta\tilde{b} - 2\tilde{\chi}, \quad \delta \tilde{g}_{03} = \tilde{\beta} \tag{3.34}$$

As in the case of a single fluid, we have possible diagonal perturbations to the metrics and the stress tensors because the perturbations are along z. The subsystem temperatures could also have the perturbations δT_1, δT_2 due to the same reason. The fluid velocities will now

be modified as

$$u^\mu = \left(\frac{1}{a} - \frac{1}{a^2}\delta a, 0, 0, \nu\right), \quad \tilde{u}^\mu = \left(\frac{1}{\tilde{a}} - \frac{1}{\tilde{a}^2}\delta\tilde{a}, 0, 0, \tilde{\nu}\right) \tag{3.35}$$

A similar procedure as before in the shear sector is done to construct the first order stress tensor from these hydrodynamic fields [7]. The equations available to solve the system are the two ward identities (3.1) and the four coupling equations (3.15 - 3.18) whose Fourier transform is taken to obtain the dispersion relation $\omega(k)$. Each of these six equations give two independent relations in the twelve fluctuations δa, $\delta\tilde{a}$, δb, $\delta\tilde{a}$, χ, $\tilde{\chi}$, β, $\tilde{\beta}$, ν, $\tilde{\nu}$, δT_1, δT_2.

The eight equations obtained from the coupling relations can be used to solve for the metric perturbations δa, $\delta\tilde{a}$, δb, $\delta\tilde{a}$, χ, $\tilde{\chi}$, β, and $\tilde{\beta}$ in terms of ν, $\tilde{\nu}$, δT_1, δT_2. These are then substituted in the four equations obtained from the ward identities. This gives a system of four linear homogenous equations in ν, $\tilde{\nu}$, δT_1, and δT_2. The existence of a non-trivial solution demands that the determinant of the 4×4 coefficient matrix of the system of equations be zero. This condition in ω and k can be solved to find the dispersion relation $\omega(k)$.

The leading behaviour of $\omega(k)$ is seen to be of the form [7]

$$\omega = ck - i\Gamma k^2 + \mathcal{O}(k^3) \tag{3.36}$$

where c is the hydrodynamic speed of sound, and Γ the attenuation coefficient.

So the critical behaviour of the sound sector modes are determined by the hydrodynamic speed and the attenuation constant. They have to be numerically solved as functions of $\gamma^{1/4}T$. The sound speed behaviour is derived in Fig 3.14 - Fig. 3.16. for different values of r, while the attenuation constant qualitatively behaves exactly like the diffusion constant solutions (one solution shows a similar criticality while the other remains constant).

The two sound mode solutions can smoothly exchange between one another which is more clear if the individual solutions are carefully observed. They seem to have discontinuities individually, but smoothly connect with the discontinuities in the other mode. The exciting result at r_c is that one mode is exactly the thermodynamically defined sound speed (3.23, Fig. 3.9.). This mode vanishes at the critical point. However the second mode does not vanish at r_c, but remains finite. This is very interesting to explore further to understand how this transport works at the critical point. In the case of the attenuation constant, like the diffusion constant in the shear sector, both modes remain finite at the critical point. One of

them is constant for all r. This is again worth studying further to understand transport at the critical point.

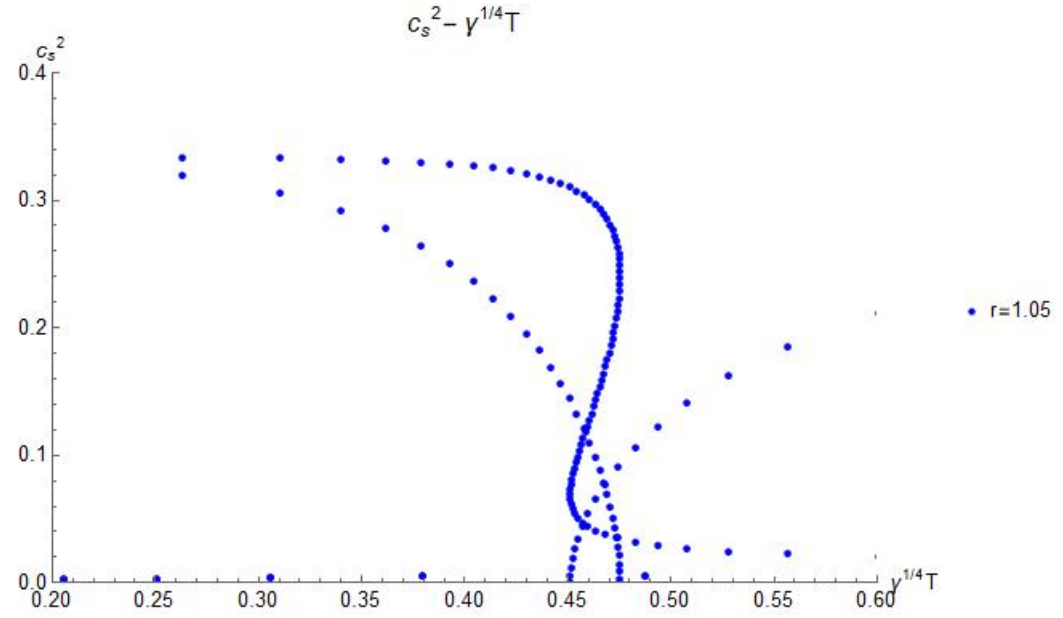

Figure 3.14: *Sound modes below r_c.* Both solutions seem to be multivalued with crossover below r_c. The few points lying close to the x-axis are from the unphysical branch.

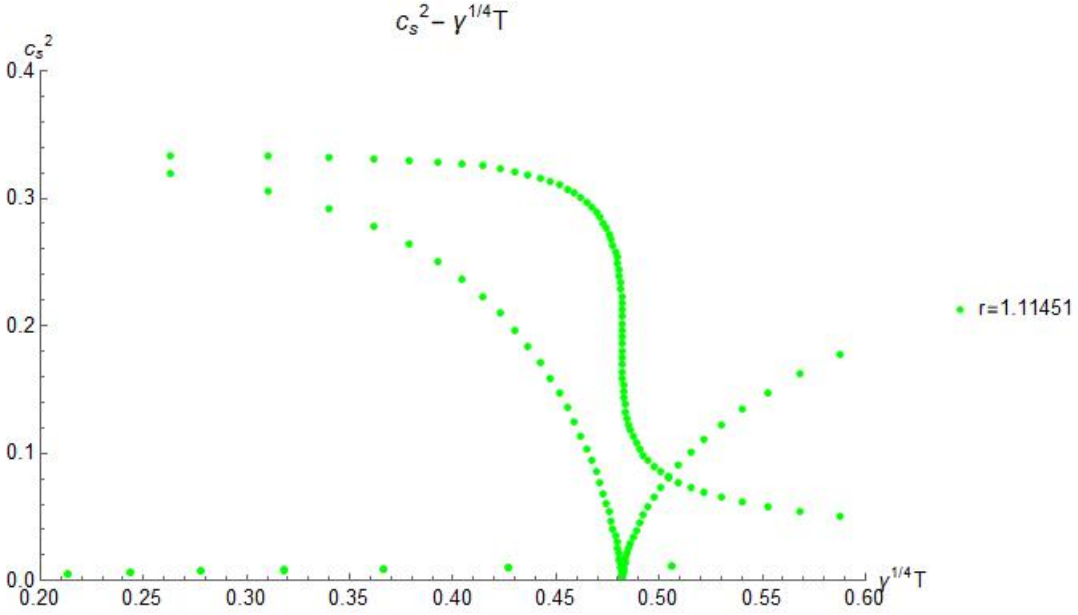

Figure 3.15: *Sound modes at r_c.* One of the solution is exactly the thermodynamic speed in Fig. 3.9. which vanishes at the critical point, while the other does not. The few points lying close to the x-axis are from the unphysical branch.

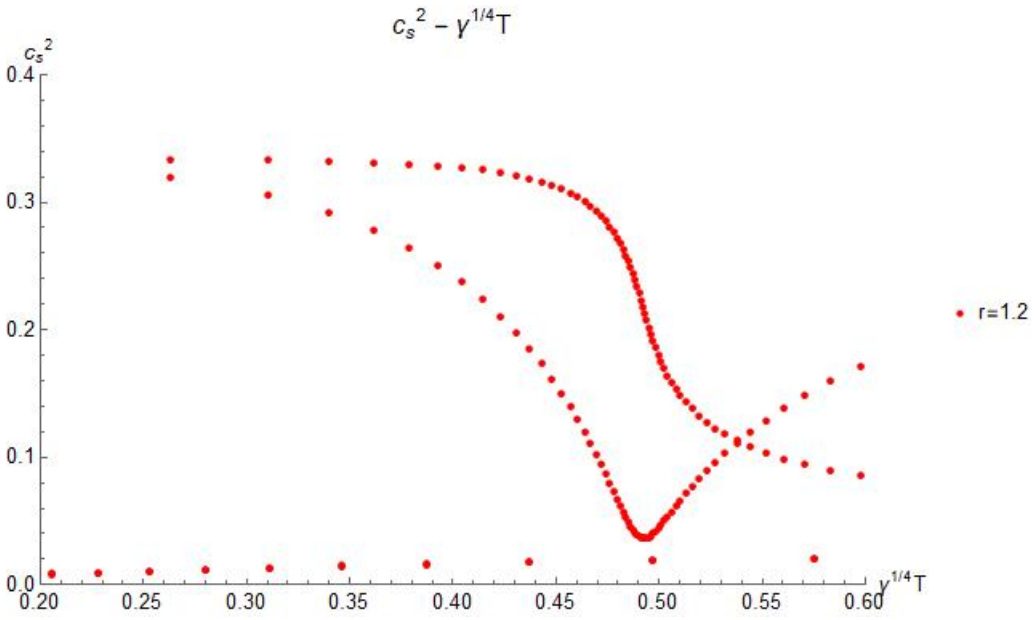

Figure 3.16: *Sound modes above r_c.* Both solutions are well behaved above r_c. The few points lying close to the x-axis are from the unphysical branch.

3.5.1 Unequal systems

So far we have only solved the system for two identical fluids. We can perform any of the above calculations for unidentical systems. For ideal fluids, in the case of sound speed, we observe a significant difference from the case of identical systems. We have computed the sound modes for two unequal systems to show that neither of the mode is the same as the thermodynamic sound. Neither vanish at the critical point, which here occurs at a different value of the coupling parameter r depending on n_1, n_2.

We no longer have $v_1 = v_2$. So all variables are analytic functions of v_1, v_2 instead of a single v. The coupling equations (3.19), (3.20) provide the total system temperature T as a function of v_1, v_2, along with a constraint equation between v_1, v_2. These two can be used together to numerically solve for v_1 and v_2 as functions of T. This in turn allows us to numerically solve for all physical quantities as a function of only T similar to the case of identical fluids.

Another difference noticed is the absence of the unphysical branch in our calculations. This is again because we have two distinct light cone velocities v_1 and v_2, unlike the case of identical fluids where $v_1 = v_2$.

The next step in developing the theory of coupled systems is to consider two MIS fluids. This provides a more accurate description of two strongly coupled subsystems. We also encounter non-hydrodynamic modes for the first time in coupled systems because of the relaxation terms in the MIS stress tensor. The behaviour of these modes near the critical point is explored in the next section. In future, it would also be interesting to find the hydrodynamic attractor for this coupled system and find its critical behaviour.

3.6 Non-hydrodynamic modes in Coupled MIS fluids

Since we have been studying coupled fluids obeying ideal hydrodynamics, we have only encountered hydrodynamic modes so far. So to study the critical behaviour of non-hydrodynamic modes, we need to consider two coupled MIS fluids which are very close to equilibrium. We add perturbations to the stress tensor and an MIS field, which obey the Ward identities (3.1) and the MIS equations (2.10) for the individual subsystems.

To compute non-hydrodynamic modes, we can treat the perturbations as functions of only time with no spatial dependence since these modes are the ones which exist in the $\mathbf{k} \to 0$ limit. Therefore there is no preferred direction for the fluctuations and hence there is no separation into different sectors for these modes. Even if we assume perturbations of the form of one of the sectors, we get identical non-hydrodynamic modes in all of them. This is seen in the case of a single MIS fluid in section 2.7.

So we can assume any particular form of perturbations for computing these modes. We assume a simple scenario with effective metric perturbations in addition to (3.12) of the form

$$\delta g_{13} = \gamma_{13}, \quad \delta \tilde{g}_{13} = \tilde{\gamma}_{13} \tag{3.37}$$

Further adding a δg_{01} term similar to the shear sector just gives a trivial solution for δg_{01}. This also happens on adding an analogous perturbation to u^μ. So u^μ is $(1/a, 0, 0, 0)$ and a similar form holds for the second subsystem also.

We also add the independent MIS fields $\Pi^{13} = \phi$, $\tilde{\Pi}^{13} = \tilde{\phi}$ to the ideal stress tensors of the respective subsystems. Upto first order in perturbations, the only modification to the

ideal stress tensor is

$$\delta T^{13} = \phi - \frac{\gamma_{13} P_1}{b^4}, \quad \delta \tilde{T}^{13} = \tilde{\phi} - \frac{\tilde{\gamma}_{13} P_2}{\tilde{b}^4} \tag{3.38}$$

Now the equations available to solve for the perturbations are the two ward identities (3.1), the two MIS equations, and the four coupling equations (3.15) - (3.18). The Ward identities are trivially satisfied, the MIS equations after fourier transform give

$$\phi \left(1 - \frac{i\tau\omega}{a}\right) - \frac{i\gamma_{13}\eta\omega}{ab^4} = 0, \quad \tilde{\phi} \left(1 - \frac{i\tilde{\tau}\omega}{\tilde{a}}\right) - \frac{i\tilde{\gamma}_{13}\tilde{\eta}\omega}{\tilde{a}\tilde{b}^4} = 0, \tag{3.39}$$

and the coupling equations give the relations

$$\gamma_{13} - \gamma\tilde{a}\tilde{b}^3\tilde{\phi} + \frac{\gamma\tilde{a}P_2\tilde{\gamma}_{13}}{\tilde{b}} = 0 \quad \tilde{\gamma}_{13} - \gamma a b^3 \phi + \frac{\gamma a P_1 \gamma_{13}}{b} = 0 \tag{3.40}$$

Solving the coupling equations (3.40) gives γ_{13}, $\tilde{\gamma}_{13}$ as functions of ϕ, $\tilde{\phi}$. This can be substituted into equations (3.39) to give a system of two linear homogenous equations in ϕ, $\tilde{\phi}$. A non-trivial solution is guaranteed only if the determinant of the 2×2 coefficient matrix for the system of equations is zero. This gives the dispersion relation for the non-hydrodynamic modes. The two solutions for identical systems are plotted below in Fig. 3.17 and Fig. 3.18. We consider $T\tau$ instead of τ since it is a dimensionless quantity.

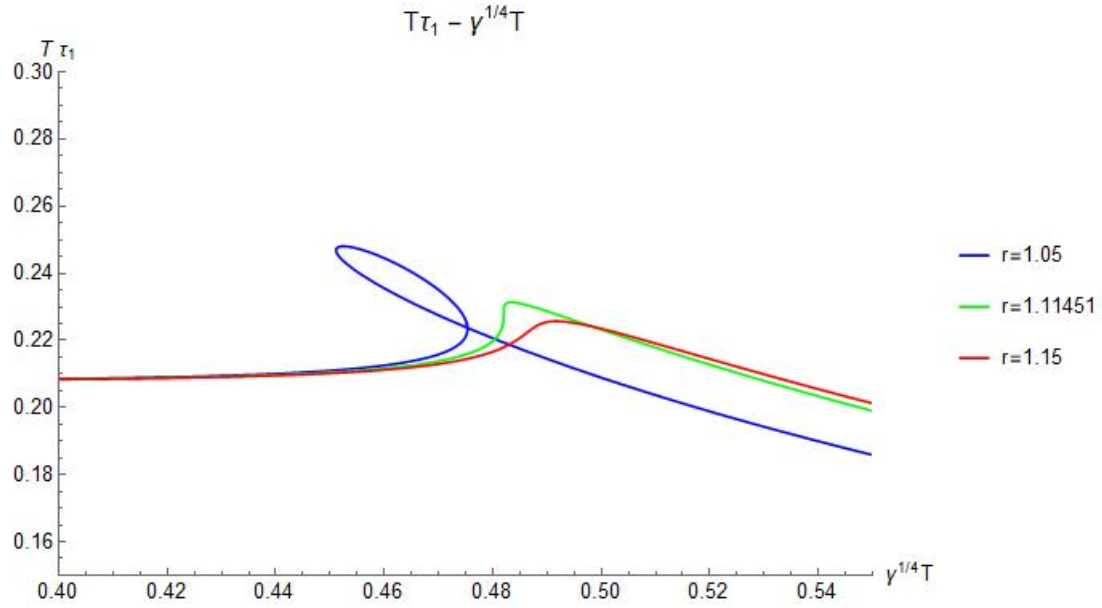

Figure 3.17: *First relaxation mode solution.* The first relaxation time has a critical point for r_c (green curve), but always remains finite.

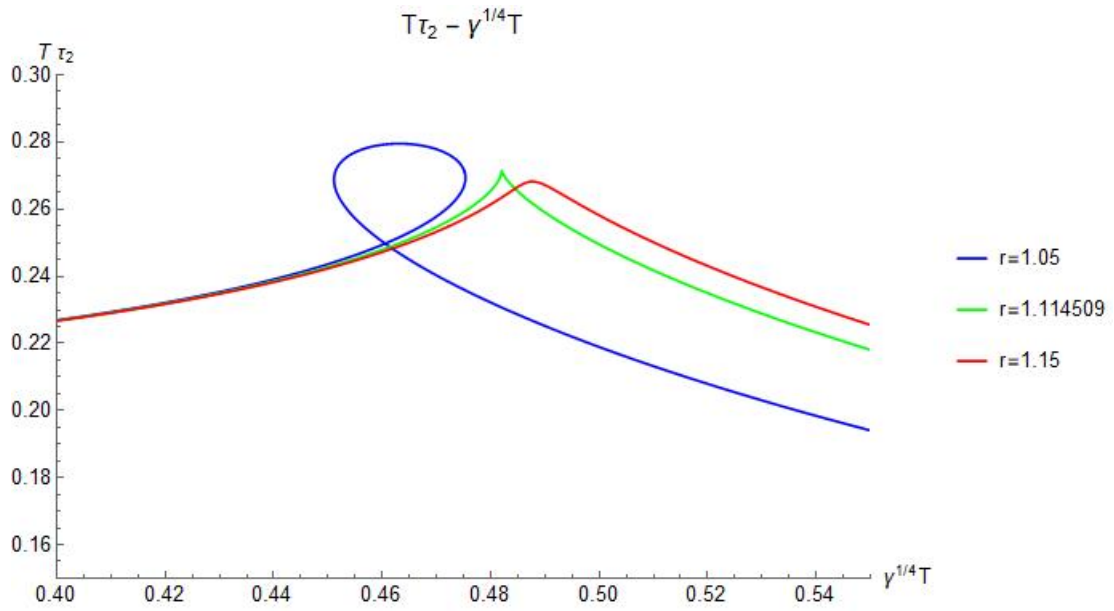

Figure 3.18: *Second relaxation mode solution.* The second relaxation time also has a critical point at r_c (green curve), but always remains finite.

We do observe critical behaviour in both modes with the blow up of first derivative at r_c for one solution, and discontinuity in the slope at r_c for the second solution. But both the solutions remain finite at the critical point. This again is interesting because we might expect the relaxation mode to be absent at the critical point because of the prevalent long-range correlations.

Chapter 4

Summary and Outlook

We have studied the very useful method of effective field theory to construct hydrodynamic descriptions of strongly interacting systems at long wavelengths. The hydrodynamic gradient expansion was studied, but shown to be acausal. The causal MIS theory adds phenomenological relaxation modes in fluids and these modes lead to the existence of hydrodynamic attractors. This result is very important in explaining the effectiveness of the MIS theory in describing the Quark-Gluon Plasma, and helps in developing an out of equilibrium theory of hydrodynamics.

We saw how the non-hydrodynamic modes arise in MIS fluids and how these lead to the decay of fluctuations near the attractor. The other approach to improving finite order hydrodynamics motivated by the necessity to cure the problem of divergent hydrodynamic gradient expansions is the mathematical process of Borel resummation. This provides a sensible result for the divergent expansion which is much better than any finite order truncation. We also saw how this procedure however leads to the exact results as obtained from the MIS formalism hence increasing our confidence in both these methods.

A more accurate description for the QGP can be constructed by coupling both strongly interacting and weakly interacting modes. Semi-holography provides a model to possibly introduce such couplings through effective metrics for the two sectors. In this approach we already observe a rich theory of critical dynamics for two strongly interacting ideal fluids.

All physical variables in the theory of coupled identical ideal fluids are analytic functions

of a single light-cone velocity, and so all these variables show a similar critical behaviour when numerically solved as functions of the total system temperature T. Their derivative with respect to T blows up or becomes discontinuous at the critical value of the coupling parameter r_c, though the function itself remains continuous. Below r_c, the functions themselves are discontinuous and thus exhibit a first order crossover by superheating or supercooling. Above r_c they remain continuous and smooth. Some variables like the entropy and diffusion constant were explicitly shown to scale exactly like v as expected $\sim |T - T_c|^{1/3}$.

To explore how propagation of modes are affected near the critical point, we computed the thermodynamic sound speed and the hydrodynamic and non-hydrodynamic modes. The thermodynamic sound vanished exactly at r_c, and one of the sound modes in the sound sector also exhibited this same behaviour in the case of identical fluids. However the diffusion constant in the shear mode, the attenuation constant in the sound mode, and the relaxation time in the non-hydrodynamic mode remained finite at r_c even though they had a critical point. The significance of these non-zero modes at the critical point has to be studied further.

To understand fluctuations near the critical point better, we need to include stochasticities since these could be large near this point. This is a direction we are currently pursuing. A renormalised theory can possibly be constructed analogous to the description for a single fluid developed in [9], and the RG flow of transport coefficients could be studied.

We hope to extend the developments in [7] and this thesis, to include couplings between kinetic theories and fluids. This would be very relevant to QGP dynamics which does show very close agreement to kinetic theory beyond the fluid regime when the interactions become weaker. What the critical point in these systems signify in the context of QGP dynamics would be important to understand. We could also study if an attractor exists for the coupled system, and how the attractor solution for the MIS subsystem affects the kinetic subsystem dynamics.

Another goal is to study the phase transition for coupled MIS fluids near the attractor for the combined system. Such an effort has been started by Dr. Ayan Mukhopadhyay and colleagues, who were able to recently derive the hydrodynamic attractor in a hybrid MIS theory. The next step is to find the critical value of the interaction parameter for this attractor and then perform further computations near it. This could show how the attractor behaves near the critical point and help find out if the critical behaviour itself is modified in the presence of the attractor.

Bibliography

[1] S. Bhattacharya, V. E. Hubeny, S. Minwalla, and M. Rangamani, *Nonlinear fluid dynamics from gravity*, JHEP **0802**, 045 (2008), arXiv:0712.2456 [hep-th].

[2] V. E. Hubeny, S. Minwalla, and M. Rangamani, *The fluid/gravity correspondence*, arXiv:1107.5780 [hep-th].

[3] G. Policastro, D. T. Son, and A. O. Starinets, *From ADS/CFT correspondence to hydrodynamics*, JHEP **09**, 043 (2002), [hep-th/0205052].

[4] G. Policastro, D. T. Son, and A. O. Starinets, *From ADS/CFT correspondence to hydrodynamics. II: Sound Waves*, JHEP **12**, 054 (2002), [hep-th/0210220].

[5] R. Baier, P. Romatschke, D. T. Son, A. O. Starinets, and M. A. Stephanov,*Relativistic viscous hydrodynamics, conformal invariance, and holography*, JHEP **0805**, 087 (2008), arXiv:0801.3701 [hep-th]. ‘

[6] M. P. Heller and M. Spaliński, *Hydrodynamics beyond the Gradient Expansion: Resurgence and Resummation*, Phys. Rev. Lett. **115** 072501 (2015), arXiv:1503.07514 [hep-th].

[7] A. Kurkela, A. Mukhopadhyay, F. Preis, A. Rebhan and A. Soloviev, *Hybrid fluid models from mutual effective metric couplings*, JHEP **08** (2018) 054, arXiv: 1805.05213 [hep-ph].

[8] C. Ecker, A. Mukhopadhyay, F. Preis, A. Rebhan and A. Soloviev, *Time evolution of a toy semiholographic glasma*, JHEP **08** (2018) 074, arXiv:1806.01850 [hep-th].

[9] P. Kovtun, *Lectures on hydrodynamic fluctuations in relativistic theories*, J. Phys. A: Math. Theor. **45** (2012) 473001, arXiv:1205.5040 [hep-th].

[10] P. Romatschke and U. Romatschke, *Relativistic Fluid Dynamics In and Out of Equilibrium - Ten Years of Progress in Theory and Numerical Simulations of Nuclear Collisions*, arXiv: 1712.05815 [nucl-th].

[11] M. Rangamani, *Gravity and Hydrodynamics: Lectures on the fluid-gravity correspondence*, Class.Quant.Grav. **26** 224003 (2009), arXiv:0905.4352 [hep-th].

[12] L. Landau and E. Lifshitz, Fluid Mechanics: Course of Theoretical Physics, Vol. 6, Butterworth-Heinemann, 1965.

[13] M. P. Heller, R. A. Janik, and P. Witaszczyk, *Hydrodynamic Gradient Expansion in Gauge Theory Plasmas*, Phys. Rev. Lett. **110** (2013) no.21, 211602, arXiv:1302.0697 [hep-th].

[14] I. Müller, *Zum Paradoxon der Warmeleitungstheorie* Z.Phys. **198** (1967) 329-344.

[15] W. Israel and J. Stewart, *Transient relativistic thermodynamics and kinetic theory*, Annals Phys. **118** (1979) 341-372.

[16] J. Bjorken, *Highly Relativistic Nucleus-Nucleus Collisions: The Central Rapidity Region*, Phys. Rev. **D 27** (1983) 140-151.

[17] R. Wald, General Relativity, Chicago, University of Chicago Press, 1984.

[18] R. Loganayagam, *Entropy current in conformal hydrodynamics*, JHEP **0805**, 087 (2008), arXiv:0801.3701 [hep-th].

[19] P. C. Hohenberg and B. I. Halperin, *Theory of dynamic critical phenomena*, Rev. Mod. Phys. **49** 435 (1997).